May 2023

Online supplementary material

Materials and methods

No statistical methods were used to predetermine sample size. Experiments were not randomised. Investigators were not blinded to allocation during experiments and outcome assessment, unless otherwise mentioned.

Submerged monolayer cell culture

According to the manufacturer's instructions, human bronchial epithelial (HBE) cells, normal HBE (NHBE) cells (Lonza, CC-2540) or diseased (COPD) HBE cells (Lonza, 00195275) (table 1 and 2) were cultured in complete BEGM (Lonza, CC-3171) with the supplement kit (Lonza, CC-4175). A549 cells (ATCC, CCL-185) were cultured in full RPMI medium with GlutaMAX (Thermo Fisher Scientific, 61870036), which contained 10% fetal bovine serum (FBS) and 1% penicillin/streptomycin. According to the manufacturer's protocol, human umbilical vein endothelial cells (HUVECs) were obtained from Cambrex (CC-2519) and maintained in EBM-2 culture (Lonza, CC-3162. Cells were harvested with accutase (PAA, L11-007), seeded at the indicated densities. Cells were washed and serum starved (BEGM [Lonza, CC-3171] without the supplement kit, or RPMI medium with GlutaMAX without FBS) and incubated at 37°C for 18–24 h.

Scratch wound healing assays in submerged monolayer cell cultures

Healthy NHBEs and COPD bronchial epithelial cells in complete BEGM or A549 cells in full RPMI medium were seeded at 5×10^5 cells/100 µL into Incucyte® Imagelock 96-well Plates (Sartorius, 4379) and incubated at 37°C for 18–24 h until confluent. Cells were then washed with PBS and serum starved overnight. The next morning cells were scratched using a WoundMaker (Sartorius, 4493), washed with PBS and

cultured in either BEBM (Lonza, CC-3171) for bronchial epithelial cells or RPMI medium with GlutaMAX for A549 cells. Both culture mediums were supplemented with 0.1% (v/v) FBS and 1% (v/v) penicillin/streptomycin. Cells were treated with 30 ng/ml of IL-33^{red}, IL-$33^{C>S}$, IL-33^{ox}, EGF or sST2 with or without 10 µg/ml of IL-33-neutralising antibody (tozorakimab), ST2-neutralising antibody, EGFR-neutralising antibody, mouse IgG1 isotype control or human IgG1 isotype control, or left untreated, before being incubated at 37°C. IncucyteZOOM or Incucyte S3 (Essen Bioscience) systems were used for wound healing imaging and analysis over a 48-h period. Relative wound density (ratio of the occupied area to the total area of the initial scratched region) was calculated through the wound healing algorithm in the Incucyte ZOOM/S3 software.

Three-dimensional ALI (air–liquid interface) cultures

Transwells containing 12 mm or 6.5 mm 0.4 µm polyester membrane inserts (Corning, CLS3460 or CLS3470) were coated with CellAdhere Type I Collagen (Stemcell, 07001) diluted once in distilled H_2O and incubated at 37°C for 1–16 h, then washed with PBS.

Lung epithelial cells from healthy controls (bronchial [Lonza, CC-2540, normal human bronchial epithelial, NHBE] or small airway [Epithelix, EP61SA]) or patients with COPD (bronchial [Lonza, 195275, diseased human bronchial epithelial, DHBE] or small airway [Epithelix, EP66SA]) were grown in four T-175 flasks in EpiX Medium (Propagenix, 276-201) for bronchial cells or small airway epithelial cell growth medium (PromoCell, C-21070) for small airway epithelial cells (see tables 1 and 2). Once confluent, cells were frozen down at 1×10^6 cells/vial at passage 2. Cells at passage 2 were plated in two T-75 flasks, grown until 80% confluent, and washed and detached using 6 mL trypsin (Lonza, CC-5034). The cell suspension was

centrifuged at 1200 RPM for 5 min and cells were resuspended in PneumaCult ALI medium (Stemcell, 05001) for bronchial cells or PneumaCult ALI-S medium (Stemcell, 05050) for small airway cells at 8×10^5 cells/mL; 0.5 mL and 0.25 mL were dispensed onto each 12 mm and 6.5 mm insert, respectively, and 1 mL or 0.5 mL of ALI medium were added into the space below the respective inserts. Cells were maintained in the appropriate ALI medium until a confluent monolayer was observed. Medium was then removed from the apical side and cells were differentiated for 3 weeks, with medium changed on the basal side every 2–3 days. Differentiation was confirmed by visually observing beating cilia and mucus production on the apical surface. After 3 weeks differentiation, ALI cultures were then incubated with the indicated agonists or antibodies for a further week during which time media and proteins were refreshed fully every 2–3 days. See table 3.

Recombinant protein production

Cloning and expression of IL-33

cDNA molecules encoding the mature component of wild-type (WT) human IL-33 (aa 112–270), UniProt accession number 095760 (IL-33^{red}), and a variant with all four cysteine residues mutated to serine (IL-$33^{C>S}$, C208S, C227S, C232S and C259S) that is resistant to oxidation were synthesised by primer extension PCR and cloned into pJexpress 411 (DNA 2.0). WT IL-33 was considered to be in its reduced form (IL-33^{red}) in 2× DPBS storage buffer before addition to culture medium. Sequences of both were modified to contain a 10× His, Avitag and Factor Xa protease cleavage site (MHHHHHHHHHHAAGLNDIFEAQKIEWHEAAIEGR) at the N-terminus. IL-33^{red} (N-terminal tagged His10/Avitag; WT) and IL-$33^{C>S}$ (N-terminal tagged His10/Avitag; WT) were generated by transforming *Escherichia coli* BL21(DE3) cells, which were cultured in autoinduction medium (Overnight Express Autoinduction System 1, Merck Millipore, 71300-4) at 37°C for 18 h, harvested by centrifugation and stored at −20°C.

Cells were resuspended in 2× DPBS containing complete EDTA-free protease inhibitor cocktail tablets (Roche, 11697498001) and 50 U/mL Benzonase nuclease (Merck Millipore, 70746-3), and lysed by sonication. Cell lysate was centrifuged at 50 000×*g* for 30 min at 4°C. IL-33 proteins were purified from the supernatant by immobilised metal affinity chromatography and further purified by size-exclusion chromatography (SEC) using a HiLoad 26/600 Superdex 75 pg column (GE Healthcare, 28989334). Peak fractions were analysed by SDS-PAGE. Fractions containing pure IL-33 were pooled and their concentrations determined by measuring absorbance at 280 nm. Final samples were analysed by SDS-PAGE. To generate untagged IL-33^{red} or IL-33$^{C>S}$, N-terminal tagged His10/Avitag IL-33 was incubated with 10 units of Factor Xa (GE Healthcare, 27084901) per mg of protein in 2× DPBS at room temperature for 1 h. Untagged IL-33 was purified using SEC on a HiLoad 16/600 Superdex 75 pg column (GE Healthcare, 28989333) with a flow rate of 1 mL/min.

Generation and purification of IL-33^{ox}

IL-33^{red} was oxidised by dilution to a final concentration of 0.5 mg/mL in 60% Iscove's Modified Dulbecco's Medium (IMDM) (with no phenol red) and 40% Dulbecco's Phosphate Buffered Saline (DPBS) and incubated at 37°C for 18 hours. Tags were cleaved from IL-33^{ox} by incubation with Factor Xa (NEB, P8010L) at a final concentration of 1 µg/50 µg of IL-33^{ox} for 120 min at 22°C. To deplete the sample of any remaining IL-33^{red}, soluble human ST2 fused to human IgG1 Fc-His6 was incubated with the sample for 30 min at 22°C. The sample was concentrated and loaded on a HiLoad 26/600 Superdex 75 pg column (GE Healthcare, 28989334) at a flow rate of 2 mL/min. Each fraction containing pure IL-33^{ox} was tested for its ability to activate EGFR (homogeneous time-resolved fluorescence [HTRF] assay in A549 cells and NHBE cells). Active fractions from batches were pooled and concentrated,

and the final concentration of the sample was determined using UV absorbance spectroscopy at 280 nm. Final product quality was assessed by SDS-PAGE, high-performance SEC and reverse-phase HPLC. Additionally, liquid chromatography-mass spectrometry (LC-MS) was performed to confirm that IL-33^{ox} was 4 daltons lighter than IL-33^{red}. The efficiency of IL-33^{ox} generation from recombinant IL-33 materials was 1.2–1.4%: 93.6 mg of initial WT IL-33 (batch no. CCH275) produced 1.13 mg of active IL-33^{ox} (1.2%); 134.4 mg initial WT IL-33 (batch no. CCH276) produced 1.9 mg of active IL-33^{ox} (1.4%).

CRISPR-Cas9 ablation of RAGE in A549 cells

A mammalian plasmid was generated containing expression vectors for red fluorescent protein (RFP), guide RNA targeted to exon 3 of *AGER* (TGAGGGGATTTTCCGGTGC) and a Cas9 endonuclease. A549 cells cultured in Ham's F-12K Nutrient Mixture (Gibco, 11765054) with 10% FBS and 1% penicillin/streptomycin were seeded at a concentration of 2×10^5 cells/mL in T-75 flasks. Cells were transfected with *AGER* guide RNA plasmid and polyethylenimine, linear 22 µg (Polysciences, 23966-2). After a 2-day incubation following the transfection, RFP-positive cells were sorted using the FACSAria Cell Sorter (BD) and loss of RAGE from A549 cells was confirmed by genomic PCR analysis.

Generation of ST2L-expressing A549 cells

A549 cells were plated at a concentration of 5×10^5 cells in a 12-well culture plate (Corning, 3513). Lentiviral particles containing ST2 (IL1RL1) (NM_016232) Human Tagged ORF Clone were purchased from OriGene (RC217503L3V, 4.1×10^4 TU/µL). Two wells of A549 cells (pool 1 and pool 2) were infected with the lentiviral particles in the presence of 1 µg/mL polybrene (Sigma, H9268). After 4 h, the RPMI medium was refreshed and a further 24 h later the cells were switched to RPMI selection

medium containing 0.5 µg/mL puromycin (Gibco, 12122530), and the cells were cultured for 48 h. Cells from pool 1 were used to generate A549 clones (1A2, 1B2 and 1B4).

Western blots and immunoprecipitation

Submerged NHBE cells or bronchial epithelial ALI cultures were lysed in lysis buffer containing LDS sample buffer (Thermo, NP0008), 10 mM $MgCl_2$ (VWR, 7786-30-3), 2.5% β-mercaptoethanol (Sigma, M6250) and 0.4 µg/mL Benzonase (Millipore, 70746), and were heated to 95°C for 5 min. The samples and protein ladder (Bio-Rad, 1610374) were run on a 4–12% SDS-PAGE gel (Thermo, NW04127BOX) in MES running buffer (Thermo, B0002). Gels were transferred onto PVDF membranes (Bio-Rad, 1704156) using a Trans-Blot Turbo (Bio-Rad). Membranes were blocked and blotted with primary antibodies. Immunoreactive bands were developed using horseradish peroxidase (HRP)-conjugated secondary antibodies (table 4) and enhanced chemiluminescence substrate (Bio-Rad, 1705062), and visualised using a C-DiGit scanner (LI-COR Biosciences).

For immunoprecipitation, cells were lysed in 1× lysis buffer (Abcam, ab152163) supplemented with 1× phosphatase/protease inhibitor cocktail (Thermo, 78440), and the protein concentration was determined by a BCA assay (Thermo, 23225). NHBE protein extracts were incubated with anti-EGFR (R&D systems, AF231) at 4°C for 2.5 h. Protein A/G magnetic beads (Thermo, 88802) were added and mixed for 1 h. Beads were collected using a SureBeads Magnetic Rack (Bio-Rad, 1614916), washed, and proteins were released by treating with LDS sample buffer (Thermo, NP0008) and Sample Reducing Agent (Thermo, NP0004) at 95°C for 5 min. Membranes were incubated with the following primary antibodies: anti-EGFR, anti-RAGE and anti-IL-33.

Binding assay

Streptavidin plates (Thermo Scientific, AB-1226) were coated with 10 µg/mL biotinylated antigen at room temperature for 1 h. Plates were washed and blocked with 1% BSA (Sigma, A9576) in PBS for 1 h, before 10 µg/mL RAGE-Fc (R&D Systems, 1145-RG) or ST2-Fc (R&D Systems, 523-ST) was added and the plates were incubated at room temperature for 1 h. EGFR-Fc (R&D Systems, 344-ER-050), 10 µg/mL in PBS, was added in the presence or absence of 10 µg/mL untagged RAGE (Sino Biological, 11629-HCCH) for 1 h. Following three washes with PBS, RAGE-Fc, ST2-Fc and EGFR-Fc were detected with 5.1 mg/mL anti-human IgG HRP (Sigma, AO170, dilution 1:10,000). Plates were washed and developed with TMB (Sigma, T0440). The reaction was quenched with 0.1 M H_2SO_4. Absorbance was read at 450 nm using Cytation Cell Imaging Gen5 software.

Immunohistochemistry 3-plex staining

Bronchial epithelial ALI epithelial cultures were fixed in 10% formalin for 24 h and embedded in paraffin. Paraffin sections (4 µm) were mounted on positively charged slides and stained using the Ventana DISCOVERY ULTRA automated slide preparation system (Roche) with a sequential 3-plex chromogenic assay.

Antigen retrieval was achieved with the cell conditioner ULTRA CC1 (Roche, 5424569001) and endogenous peroxidase was blocked with DISCOVERY Inhibitor (Roche, 7017944001) for 12 min. For basal cell staining, anti-p63 (clone 4A4) (Roche, 790-4509: ready to use format) was applied for 24 min at 36°C and cells were visualised after 12 min of incubation with anti-mouse HQ (Roche, 7017782001) and anti-HQ HRP (Roche, 7017936001). Cells were incubated with the DISCOVERY Purple Kit (Roche, 07053983001) for 12 min.

Slides were exposed to an antibody denature step (92°C for 24 min) with ULTRA CC2 (Roche, 5424542001). For ciliated cell staining, anti-tubulin (Abcam, ab24610) was diluted in Antibody Diluent (Dako, S3022) to a final concentration of 0.05 µg/mL and was applied for 16 min. Staining was detected with mouse OmniMap anti-Ms HRP for 8 min (Roche, 5269652001) and visualised using the DISCOVERY Teal HRP Kit (Roche, 82544338001).

An additional antibody denaturation step was performed with CC2 before staining with a cocktail of 1.1 µg/mL rabbit anti-MUC5AC and 7 µg/mL rabbit anti-MUC5B (Abcam, ab198294 and ab87376, respectively), which was applied for 20 min. Cells were visualised after applying anti-rabbit NP (Roche, 7425317001) for 4 min, anti-NP-AP for 8 min (Roche, 7425325001) and then the DISCOVERY Yellow Kit (Roche, 7698445001) for 20 min.

Stained slides were counterstained with Hematoxylin II for 8 min (Roche, 5277965001) and bluing reagent for 4 min (Roche, 5266769001), rinsed with dishwashing detergent, dehydrated with a graded series of ethanol and xylene, and mounted with permanent mounting media.

Immunohistochemistry images were analysed in HALO v3.1 (Indica Labs); they were first annotated manually to exclude out of focus areas and regions of tissue damage. A random forest classifier was trained to recognise the epithelium and separate it from the transmembrane and glass slide background. For cilia area quantification, another random forest classifier was trained for coarse detection of tubulin staining, followed by fine detection using the Area Quantification v2.1.7 algorithm; this algorithm was also used for mucin area quantification. For basal (p63-positive) cell

counting, the CytoNuclear 2.0.9 algorithm (Indica Labs) was used to segment cells based on nuclear staining; basal cells were further detected by counting p63-positive nuclei. All quantification methods were validated against human recognition and had more than 90% accuracy.

Multiplex immunofluorescence staining and analysis

Bronchial epithelial ALI cultures from healthy and COPD donors were fixed in 10% neutral buffered formalin for 24 h and embedded in paraffin. Paraffin sections (4 µm) were mounted on positively charged slides and stained on the Leica BOND Rx platform with a multiplex immunofluorescence assay. Antigen retrieval was performed with BOND Epitope Retrieval Solution 1 (Leica, AR9961) for 20 min and endogenous peroxidase was blocked with Novocastra Peroxidase Block (Leica, RE7101) for 20 min.

Anti-MUC5AC (Thermo, MA1-21907) used at 0.0015 µg/mL in BOND primary antibody diluent (Leica, AR9352) was applied for 60 min at room temperature and visualised with a two-step polymer detection system: Polink-2 HRP polymer enhancer (10 min) and Polink-2 HRP polymer detector (10 min) (GBI, D41-110). This was followed by incubation with Opal 690 (Akoya Biosciences, FP1496A) diluted 1:200 in Plus Amplification buffer (Akoya Biosciences, FP1498) for 10 min.

The sections underwent an antibody denature step (95°C for 20 min) using BOND Epitope Retrieval Solution 1 (Leica, AR9961) and were incubated with anti-MUC5B (Abcam, ab87376) used at 0.025 µg/mL diluted in BOND primary antibody diluent (Leica, AR9352), for 30 min at room temperature. Detection was done using a two-step polymer detection system: Polink-2 HRP polymer enhancer (10 min) and Polink-2 HRP polymer detector (10 min) (GBI, D41-110). This was followed by incubation

with Opal 570 (Akoya Biosciences, FP1488A) diluted 1:150 in Plus Amplification buffer (Akoya Biosciences, FP1498) for 10 min.

The sections underwent an additional antibody denaturation step with BOND Epitope Retrieval Solution 1 (Leica, AR9961) and were incubated with anti-E-cadherin (4A2) (CST, 14472) used at 0.25 µg/mL diluted in BOND primary antibody diluent (Leica, AR9352), for 30 min at room temperature. Detection was done using a two-step polymer detection system: Polink-2 HRP polymer enhancer (10 min) and Polink-2 HRP polymer detector (10 min) (GBI, D41-110). This was followed by incubation with Opal 520 (Akoya Biosciences, FP1487A) diluted 1:50 in Plus Amplification buffer (Akoya Biosciences, FP1498) for 10 min.

An additional antibody denaturation step with BOND Epitope Retrieval Solution 1 (Leica, AR9961) was performed for 20 min at 95°C. The slides were stained with DAPI (Akoya Biosciences, FP1490) diluted in BOND wash solution (Leica, AR9590) for 10 min at room temperature. Slides were then rinsed with deionised water and mounted with ProLong Diamond antifade mounting media (Thermo, P36965) before being scanned with Akoya Vectra Polaris.

Immunofluorescence images were analysed in Visiopharm software (version 2020.08). Out of focus and disrupted tissue areas were manually excluded from the image quantification pipeline. A Bayesian classifier was trained to outline the tissue areas from the background, and a convolutional neural network (DeepLabv3+) was trained to segment the mucin areas within the outlined tissue areas. Both models were trained via supervised learning and the segmentation results were validated against human recognition.

FACS analysis

Following 7 days of treatment, 4-week-old healthy control or COPD bronchial epithelial ALI cultures on 6.5 mm inserts were analysed by flow cytometry. Then, 150 µL trypsin (Lonza, CC-5034) was added to apical and basolateral compartments, and cultures were incubated for 30 min. ALI cultures were mechanically dissociated by gentle pipetting. The cell suspension was transferred to a U-shaped 90-well plate, and cells were counted and centrifuged at 1200 RPM at 4°C for 5 min.

Cells were stained with viability dye (Thermo, 65-0865-14, diluted 1:2,000), then 200 µL of fixation and permeabilisation solution (Thermo, 00-5123 and 00-5223) were added and the cells were kept for 40 min on ice. Cells were centrifuged at 1200 RPM at 4°C for 5 min, resuspended in 300 µL permeabilisation solution (Thermo, 00-8333) and seeded at 5×10^4 cells/well. Cells were centrifuged again, resuspended in 50 µL permeabilisation solution and stained for 30 min on ice with the following antibodies: anti-MUC5AC (Abcam, ab3649, 1:400), anti-MUC5B (Abcam, ab105460, 1:800), AF488 isotype (BioLegend, 400109, 1:400) and AF647 (BioLegend, 400130, 1:800). Anti-MUC5AC was coupled to AF488 (Abcam, ab236553) and anti-MUC5B was coupled to AF647 (Abcam, ab269823) using Lightning-Link kits (Abcam) according to the manufacturer's instructions. Data were acquired on a BD FACSymphony instrument and analysed using FlowJo software.

Phospho-ELISAs and proliferation assays

A549 cells were seeded at 5×10^5 cells/100 µL for phospho-ELISAs or 2 x 10^3 cells/100 µL for proliferation assays in 96-well plates. Following incubation at 37°C for 18–24 h, cells were washed twice and serum starved for 18–24 h. Cells were incubated with indicated antibodies for 30 min and then with indicated agonists for 10 min before lysis and detection according to the manufacturer's instructions (phospho-

ELISAs: p-ERK1/2 [Thermo, 85-86012-11], p-STAT5 [Thermo, 85-86112-11]; proliferation: CellTiter-Glo 2.0 cell viability assay [Promega, G9242]).

IL-6 ELISA

A549 cells or HUVECs were seeded at 5×10^5 cells/100 µL in 96-well plates. Cells were incubated with indicated antibodies for 30 min and then with indicated agonists for 20 h (table 5). Supernatants were analysed for IL-6 release using a Duoset ELISA (R&D Systems, DY206) according to the manufacturer's protocol.

MUC5AC ELISA

Mucin5AC ELISAs were purchased from Novus Biologicals (NBP2-76703). Apical supernatants were collected from ALI cultures following a 30 min incubation at 37°C with 0.2 mL PBS in the apical region per 24-well transwell culture. Apical washes were diluted 1:200 with kit diluent and the ELISA was performed according to manufactures instructions.

Phosphorylation arrays

MAP kinase phosphorylation antibody array kits (Abcam, ab211061) and RTK phosphorylation antibody array kits (Abcam, ab193662) were used according to the manufacturer's instructions. Briefly, submerged NHBE cells plated in a 6-well dish were serum starved for 18–24 h, treated with 30 ng/mL of IL-33^{red}, IL-$33^{C>S}$, IL-33^{ox} or EGF, or left untreated, and incubated at 37°C for 10 min. Cells were washed and supplemented with lysis buffer. Protein extracts were centrifuged at 14 000 RPM at 4°C, and protein concentrations were determined using the BCA protein assay (Thermo, 23225), for which 250 µg of total protein was used per array membrane. Membranes were visualised using a LI-COR C-DiGit scanner and quantified using Image Studio Lite software.

HTRF assay

Submerged NHBE cells or A549 cells were plated at 5×10^5 cells/100 µL in a 96-well plate, incubated at 37°C for 18–24 h, then washed with PBS and serum starved for a further 18–24 h. Cells were stimulated with increasing concentrations of ligands before being returned to 37°C for 10 min. Cells were lysed using 50 µL of lysis buffer, then the assay was carried out according to the manufacturer's instructions (HTRF kit; Cisbio, 64EG1PEH). Time-resolved fluorescence was read at 620 nm and 665 nm using an EnVision plate reader (Perkin Elmer), and data were analysed by calculating the 665:620 nm ratio. EC_{50}s were determined by curve fitting using a four-parameter logistic equation in GraphPad Prism software.

qPCR

Following 7 days of treatment, 4-week-old healthy or COPD ALI (bronchial or small airway epithelial) cultures on 6.5 mm inserts were lysed for RNA analysis. Each ALI apical surface was incubated at 37°C for 30 min with 200 µL PBS. Direct-zol RNA Miniprep kits (Zymo Research, R2050) were used for RNA extraction. For submerged cultures (A549 cells, HUVECs and NHBE cells), the RNeasy Mini Kit (Qiagen, 74104) was used. cDNA was synthesised using the High-Capacity RNA-to-cDNA Kit (Thermo, 4388950).

For RT-qPCR, 4 µL cDNA, 5 µL TaqMan Fast Advanced Master Mix (Thermo, 4444557), 0.5 µL MUC5AC FAM probe (Thermo, Hs01365616_m1) or MUC2 (Thermo, Hs00894041_g1) or CST1 (Thermo, Hs00606961_m1) or ST2 long (Thermo, Hs00249389_m1) or ST2 short (Thermo, Hs01073297_m1), and 0.5 µL GAPDH VIC probe (Thermo, Hs02786624_g1) were added to a MicroAmp EnduraPlate (Thermo, 4483273). Plates were sealed and briefly centrifuged before

analysis using a QuantStudio 7 Flex Real-Time PCR system (Thermo). ΔΔCT was calculated by normalising data to an untreated control.

Bulk RNA sequencing

RNA extracted from bronchial epithelial ALI cultures was processed externally by Source BioScience (Cambridge, UK). The library was prepared using the Illumina mRNA stranded kit. Sequencing was performed on an Illumina NovaSeq 6000 System to generate 30M 150-base-pair paired-end reads. RNA libraries were prepared in accordance with the NEBNext Ultra II Directional RNA Sample Preparation Protocol for Illumina Paired-End Multiplexed Sequencing.

Sequenced libraries were checked for quality using MultiQC [1] based on STAR [2] alignment against the GRCh38 ensembl (v100) human genome. Adapter trimming was performed using NGmerge [3], and Salmon [4] was used for gene expression quantification using GRCh38 ensembl (v100) as a reference. The bioinformatics workflow was organised using Nextflow [5] and Bioconda software management tools [6]. Differential expression analysis was performed in R using the DESeq2 [7] package with “apeglm”[8] fold change shrinkage. The Benjamini–Hochberg method was used for multiple correction of p-values [9]. Volcano plots showing the fold change and q-value were created using Spotfire (TIBCO) data analysis software. Gene Set Variation Analysis (GSVA) [10] was used to calculate samplewise gene set enrichment scores for the generated signatures in public COPD patient gene expression data sets GSE37147 [11], GSE11784 [12] and GSE47460 [13]. Calculations were performed using the GSVA package in R. Patient groups were compared according to disease and smoking status for gene sets GSE37147 and GSE11784, and according to COPD severity by GOLD stage for GSE47460. Significance was calculated using one-way ANOVA, followed by *post hoc* pairwise

comparisons with Tukey's honest significant difference test conducted in Prism 9 (GraphPad). Linear regression of GSVA enrichment scores versus predicted FEV_1 (%) from patients with COPD in GSE47460 was performed using TBCO Spotfire.

Single-cell RNA sequencing

Single-cell suspensions of bronchial epithelial ALI cultures were generated as described in the FACS analysis section, washed twice with PBS/0.04% BSA and resuspended at 900 cells/µL. Cells were mixed with reagents from Chromium Next GEM Single Cell 3' GEM Kit v3.1 (10x Genomics, 1000123), as per the manufacturer's instructions. Both the sample mix and capture beads from Chromium Next GEM Single Cell 3' Gel Bead Kit v3.1 (10x Genomics, 1000122) were loaded onto the microfluidic chip – Chromium Next GEM Chip G (10x Genomics, 2000177) – aiming to capture 8000 cells per sample. The chip was run on a Chromium Single Cell Controller (10x Genomics, GCG-SR-1) for single-cell partitioning and barcoding, and cDNA was prepared from the barcoded cells using Chromium Next GEM Single Cell 3' GEM Kit v3.1 (10x Genomics, 1000123). Data were aligned to GRCh38-3.0.0 human reference genome using CellRanger v3.0.1 (10x Genomics). A quality control check of cDNA was performed using NGS high sensitivity assay (Agilent Technologies, DNF-474-0500) on Fragment analyzer (Agilent Technologies). Single cell libraries were prepared using Chromium Next GEM Single Cell 3' Library Kit v3.1 (10x Genomics, 1000157), as per manufacturer's guidelines. QC was performed on the libraries using NGS high sensitivity assay (Agilent Technologies, DNF-474-0500) on Fragment analyzer (Agilent Technologies) and dsDNA HS assay (Invitrogen, Q32851) on Qubit fluorometer (Invitrogen). Appropriately diluted and pooled libraries were loaded for sequencing on Novaseq (Illumina), on 3 flow cells, 2x NovaSeq 6000 S1 Reagent Kit, 100 cycles (Illumina, 20028319) and 1x NovaSeq 6000 S2 Reagent Kit, 100 cycles (Illumina, 20028316), as per 10x Genomics recommendations for

sequencing read, type and depth. Normalisation and downstream analyses were performed using the Seurat v3.2.3 [14] package in R v3.6.3. Raw counts were normalised and scaled using the Seurat functions *NormalizeData* and *ScaleData* (default parameters). Uniform Manifold Approximation and Projection (UMAP) dimensionality reduction was obtained by applying Seurat's *RunUMAP* function considering the top 2000 most variable genes, and the 25 first principal components (PCAs) were obtained using Seurat's *RunPCA* function. For the healthy donor (n=3), cell clustering was performed by applying Seurat's functions *FindNeighbors* and *FindClusters*. A resolution of 0.5 was applied, as this refined a cluster containing goblet cell identity. Clusters that showed high proximity in the phylogenetic tree obtained using *BuildClusterTree* were merged. Cell cluster markers were obtained with Seurat's *FindAllMarkers* function (non-parametric Wilcoxon rank sum test) and used for cluster annotation. Cell types were annotated manually based on the highly expressed genes for each cluster and known epithelial airway cell markers (supplementary figure S5 and supplementary table S1) [15-19]. Data from COPD donors were analysed separately (n=3), using the same functions applied for the health donors. Clustering was performed with Seurat's resolution 0.6, merging clusters with high similarity. The healthy donor was used as the reference to project cell annotations onto the COPD donors (n=3) with Seurat's *TransferData* function and comparing markers between datasets. All differential gene expression analyses between distinct treatments were performed using non-parametric Wilcoxon rank sum tests using the Seurat functions *FindMarkers* and *FindAllMarkers*. Genes considered to be differentially expressed showed log-fold change cut-offs of 0.5 and adjusted p-values for multiple testing below 0.001 (Bonferroni correction).

Mass spectrometry

Anti-EGFR antibodies, 100 µg (R&D systems, AF231), were incubated with 40 mg Dynabeads (Thermo, 14311D), covalently coupled according to the manufacturer's instructions, then resuspended in PBS at 30 mg/mL and stored at 4°C.

Submerged NHBE cells (Lonza, CC-2540) were seeded at 1×10^6 cells/15 cm dish (Thermo, 157150) and maintained in complete BEGM (Lonza, CC-3171) for 30 days with a change of medium every 3 days until confluent. Cells were then washed twice with PBS and serum starved at 37°C for 18–24 h.

Cells were treated with medium alone (unstimulated control), 30 ng/mL IL-33^{red}, 30 ng/mL IL-33^{ox} or 30 ng/mL EGF, before being incubated at 37°C for 10 min, then washed twice in ice-cold PBS and lysed with 1 mL lysis buffer per dish (Abcam, ab152163) containing phosphatase and protease inhibitors (Thermo, 78440). Cells were scraped into lysis buffer and centrifuged at 14 000 RPM at 4°C. Protein concentration was determined using a BCA assay kit (Thermo, 23225) and protein extracts were normalised to 3 mg/mL with lysis buffer. Total protein extract of 6 mg was incubated with 100 µL anti-EGFR Dynabeads (described above) and mixed at 4°C for 5 h. Dynabeads were immobilised using a SureBeads Magnetic Rack (Bio-Rad, 1614916). Protein extract was washed five times with 50 mM Tris-HCl pH 7.5, 0.5% Triton X-100, 0.3 M NaCl. Beads were washed 10 times with a different wash buffer (50 mM Tris-HCl pH 7.5). RapiGest 1% (w/v) (Waters, 186001861) in 50 mM Tris-HCl pH 8.0 was added to the beads and these were heated at 60°C for 10 min. The supernatant was collected and 100 µL 50 mM Tris-HCl pH 8.0 was added to the resin and mixed before it was combined with the first elution. TCEP (Sigma, 646547) was added to yield a final concentration of 5 mM, and the sample was heated at 60°C for 10 min.

Eluates were alkylated by the addition of iodoacetamide (Sigma, 16125) to 10 mM in the dark at room temperature for 20 min. Alkylation was quenched by the addition of DTT (Sigma, D5545) to 10 mM. Tris-HCl 50 mM pH 8.0 was added to give a final sample volume of 500 µL. Trypsin (Promega, V5111), 0.5 µg, was added and samples were digested at 30°C overnight on a shaking platform at 400 RPM. Samples were acidified with trifluoroacetic acid (Sigma, 302031) to a final concentration of 2.0% (v/v) and incubated at 37°C for 1 h. Samples were centrifuged at 14 000 RPM for 30 min and the supernatant was collected. Samples were processed through C18 columns (Thermo, 87784) according to the manufacturer's instructions and dried using a speed-vac before being stored at −20°C. Samples were analysed by peptide mass fingerprinting mass spectrometry with scaffold software at the Medical Research Council Protein Phosphorylation and Ubiquitylation Unit, University of Dundee, UK.

NF-κB translocation

Cells were plated into 96-well plates at 1×10^4 cells/well and incubated with the indicated antibodies for 30 min before indicated agonists were added for another 30 min. Cells were fixed with 10% neutral buffered formalin (Sigma, HT5011), permeabilised with PBS/0.1% Triton X-100 and stained with NF-κB p65 (Thermo, PA5-16545), anti-rabbit AF488 (Invitrogen, 35552) and Hoechst 33342 dye (Thermo, 62249). Plates were analysed for nuclear NF-κB p65 translocation using a Cytation 5.

Immunohistochemistry 1-plex staining

Paraffin sections (3 µm) were mounted on FLEX IHC microscope slides (Dako, K8020, Agilent) and subjected to heat-induced epitope retrieval in a PT Link pre-

treatment module (Dako, Agilent) in Tris/EDTA (pH 9) before immunohistochemical staining. Tissue sections were blocked with EnVision FLEX peroxidase blocking reagent (Dako, Agilent), incubated with 2.5 µg/mL mouse anti-human IL-33 antibody (Enzo Life Sciences, ALX-804-840-C100) for 60 min at room temperature, and incubated with goat anti-mouse secondary antibodies conjugated to an HRP-conjugated polymer (EnVision FLEX, Agilent) and diaminobenzidine for visualisation. Nuclei were counterstained with Mayer's hematoxylin. Sections were dehydrated through ethanol series, cleared in xylene and mounted with Pertex (HistoLab). Stained slides were digitised using an Olympus VS200 SLIDEVIEW scanner.

In situ hybridisation 1-plex and 2-plex staining

Target mRNA was visualised using the RNAscope 2.5 FFPE Red Assay Kit (Advanced Cell Diagnostics) according to the manufacturer's instructions. Briefly, paraffin sections were deparaffinised through a series of alcohol and xylene baths, incubated with endogenous enzyme block for 10 min, boiled in target retrieval solution for 15 min and treated with protease for 15 min, followed by target probe hybridisation for IL-33, EGFR and IL-33 or EGFR and RAGE (Hs-IL-33, 400111; Hs-EGFR, 310061-C2; Hs-AGER, 470121). The bacterial gene *DapB* (310043) was used as a negative control probe. For 1-plex staining, the housekeeping gene *PPIB* (Hs-PPIB, 313901) was used as a positive control probe, and for 2-plex staining, *PPIB* and *POLR2a* (2-plex positive-Hs, 321641) were used as positive control probes. Target mRNA was amplified and visualised (1-plex: red chromogen; 2-plex: red [EGFR] and green [IL-33 and RAGE] chromogen). Nuclei were detected with hematoxylin. Finally, tissue sections were dehydrated and mounted under glass coverslips using Pertex (Histo lab). Stained slides were digitalised using an Olympus VS200 SLIDEVIEW scanner.

Statistical analysis

Statistical analyses were conducted using R (v.4.0.2; Vienna, Austria) or Prism 9 (GraphPad Software, San Diego, CA, USA). Data are presented as mean with standard error of the mean. A non-parametric Kruskal–Wallis test with multiple comparisons was used for comparisons between more than two groups, unless otherwise indicated. A significance threshold of 0.05 was used for *p* values. All experiments are represented by several biological replicates or independent experiments, unless otherwise mentioned. Box plots were generated using the following parameters: horizontal black lines with each box present median values; boxes extend from 25th to 75th percentiles of values; whiskers extend to a maximum of 1.5× the interquartile range (75th percentile–25th percentile) beyond the boxes; lowest dots are minimum values and highest dots are maximum values for each box. All experiments are represented by several biological replicates or independent experiments, unless otherwise mentioned. The number of replicates per experiment is indicated in the legends. The quantitative Venn diagram of mass spectrometry data was created using the *Bioinformatics & Evolutionary Genomics* web tool (https://bioinformatics.psb.ugent.be/cgi-bin/liste/Venn/calculate_venn.htpl). All western blots, co-immunoprecipitation experiments, FACS analyses, ELISAs and RT-qPCRs were independently replicated at least twice with similar results. No statistical methods were used to predetermine sample size.

Methods tables

Table 1 Human bronchial epithelial cells purchased from Lonza

Cells	Lonza catalogue number	ID	Pathology	Smoking history	Medication related to airway disease
COPD DHBE	195275	630389	COPD	Yes	Unknown
COPD DHBE	195275	32336	COPD	Yes	Albuterol
COPD DHBE	195275	430905	COPD	Yes	Unknown
COPD DHBE	195275	18TL095116	COPD	Yes	Unknown
COPD DHBE	195275	362792	COPD	Yes	Unknown
COPD DHBE	195275	409276	COPD	Yes	Inhaler and oxygen
COPD DHBE	195275	415058	COPD	Yes	Unknown
COPD DHBE	195275	636518	COPD	Yes	Albuterol, Prednisone, Mucinex
COPD DHBE	195275	239784	COPD	Yes	Unknown
COPD DHBE	195275	436083	COPD	Yes	Spiriva & Ventolin
NHBE	CC-2540	630564	Healthy	No	N/A
NHBE	CC-2540	633427	Healthy	No	N/A
NHBE	CC-2540	543643	Healthy	No	N/A
NHBE	CC-2540	608196	Healthy	No	N/A
NHBE	CC-2540	628080	Healthy	No	N/A
NHBE	CC-2540	543643	Healthy	No	N/A
NHBE	CC-2540	18TL012118	Healthy	No	N/A
NHBE	CC-2540	382850	Healthy	No	N/A

NHBE	CC-2540	501936	Healthy	No	N/A

Table 2 Human small airway epithelial cells purchased from Epithelix

ID	Pathology	Smoking history
SA069301	Healthy	No
SA068001	Healthy	No
SA067101	Healthy	No
SA037201	Healthy	No
SA070202	COPD	No
SA066802	COPD	Yes
SA066702	COPD	Yes
SA062502	COPD	Yes

Table 3 Antibodies/binding proteins used in cell culture assays

Antibody/protein	Identifier	Host species	Supplier
hIgG1	NIP228_ SP14-266	Human	AstraZeneca
Tozorakimab (anti-IL-33)	SP15-124	Human	AstraZeneca
gIgG1	AB-108-C	Goat	R&D systems
mIgG1	mNIP228_ SP14-108	Mouse	AstraZeneca
Anti-ST2	Ab1440361	Mouse	AstraZeneca
Anti-RAGE	M4F4	Mouse	AstraZeneca
Anti-EGFR	LA1, 05-101	Mouse	Millipore
Anti-ST2	AF523	Goat	R&D Systems
Anti-IL-4R	MAB230	Mouse	R&D Systems
Anti-IL-13	MAB213	Mouse	R&D Systems
Anti-EGF	MAB236	Mouse	R&D Systems
RAGE-FC protein	1145-RG	Human	R&D Systems
sST2 protein	523-ST	Human	R&D Systems

Table 4 Secondary antibodies used in western blots and immunoprecipitation assays

Epitope	Company	Cat. #	Dilution
EGFR	Cell Signaling Technology	4267	1:1000
p-EGFR Y1068	Cell Signaling Technology	3777	1:1000
p-EGFR Y1173	Cell Signaling Technology	4407	1:1000
p-EGFR Y845	Cell Signaling Technology	6963	1:1000
p-EGFR Y992	Cell Signaling Technology	2235	1:1000
p-PLCγ	Cell Signaling Technology	14008	1:1000
p-AKT S473	Cell Signaling Technology	4060	1:1000
p-STAT5	Cell Signaling Technology	9314	1:1000
p-JNK1/2	Cell Signaling Technology	4668	1:1000
p-ERK1/2	Cell Signaling Technology	4370	1:1000
p-p38 MAPK	Cell Signaling Technology	9211	1:1000

P38 MAPK	Cell Signaling Technology	9212	1:1000
IRAK1	Cell Signaling Technology	4504	1:1000
p-NF-κB (p105)	Cell Signaling Technology	4806	1:1000
GAPDH	Cell Signaling Technology	5174	1:1000
RAGE	Cell Signaling Technology	6996	1:1000
Anti-rabbit HRP secondary	Cell Signaling Technology	7074	1:10 000
IL-33	R&D Systems	AF3625	1:1000
ST2	R&D Systems	AF523	1:1000
Anti-goat HRP secondary	R&D Systems	HAF017	1:10 000

Table 5 Agonists used in ELISAs

Agonist	Supplier	Identifier	Concentration used in experiments unless stated otherwise (ng/mL)
IL-33^{ox} (wild-type form that has been oxidised causing the formation of two disulphide bonds between four cysteine residues)	AstraZeneca	RD15, CCH275 and CCH276	30
IL-33$^{C>S}$ (a mutant form of IL-33 in which all four cysteines (C208, C227, C232 and C259) have been mutated to serine, preventing the formation of disulphide bonds and making it more resistant to oxidation)	AstraZeneca	11/12/2015	30
IL-33^{red} (wild-type form of IL-33 in a reduced state that does not contain disulphide bonds)	AstraZeneca	07/24/2015	30
EGF	R&D Systems	236-EG-200	30
TGFα	R&D Systems	239-A-100	Titration
HB-EGF	R&D Systems	259-HE-050/CF	Titration

Amphiregulin (AREG)	R&D Systems	262-AR-100/CF	Titration
Betacellulin/BTC	R&D Systems	261-CE-010/CF	Titration
Epiregulin	R&D Systems	1195-EP-025/CF	Titration
Epigen	R&D Systems	6629-EP-025/CF	Titration
HMGB1	R&D Systems	1690-HMB-050	Titration
S100A8/A9	R&D Systems	8226-S8-050	Titration
S100A12	R&D Systems	1052-ER-050	Titration
S100B	R&D Systems	1820-SB-050	Titration
IL-13	R&D Systems	213-ILB	10

Supplementary tables and figures

Supplementary table S1 Mass spectrometric analysis showing immunoprecipitation of EGFR in the presence of IL-33^{ox}

		IL-33^{red}	IL-33^{ox}	EGF
Protein	Size	Total Unique Peptide Count	Total Unique Peptide Count	Total Unique Peptide Count
		n = 3	n = 3	n = 3
AP2A1	108 kDa	0	20	14
AP2A2	104 kDa	0	16	10
SHC1	63 kDa	0	15	17
SHC1	63 kDa	0	15	17
AP2B1	105 kDa	0	15	16
AP2B1	105 kDa	0	14	16
IL33	31 kDa	0	11	0
AGER	43 kDa	0	11	0
AP2M1	50 kDa	0	10	11
FASN	273 kDa	0	8	3
AP1B1	105 kDa	0	7	7
FARSA	58 kDa	0	6	5
ATAD3B	73 kDa	0	5	8
AP2S1	17 kDa	0	5	4
CBLB	109 kDa	0	5	4
EPN1	60 kDa	0	5	3
EPN1	60 kDa	0	5	3
GSN	86 kDa	0	5	3
TGFBI	75 kDa	0	4	6
TNC	241 kDa	0	4	4
MMP14	66 kDa	0	4	0
EPHB1	110 kDa	0	3	0
ATP1A2	112 kDa	0	3	0
ATP6V0A	96 kDa	0	3	10
ATP6V1A	68 kDa	0	3	4
HIST1H4A	11 kDa	0	3	0
MFGE8	43 kDa	0	3	3
RPLP2	12 kDa	0	3	0
37500	41 kDa	0	3	0
LMO7	193 kDa	0	3	5
ATP6V0D	40 kDa	0	3	5
SDCBP	32 kDa	0	3	0
ITGA6	127 kDa	0	3	7
SOS2	153 kDa	0	3	2
TNK2	115 kDa	0	0	4
EXPH5	223 kDa	0	0	3
SVIL	248 kDa	0	0	3
APOD	21 kDa	6	0	0
PCBP2	39 kDa	3	0	0
RPN2	69 kDa	3	0	0
ALDH1B1	57 kDa	3	0	0
OS9	76 kDa	3	0	0
TPM4	29 kDa	3	0	0

Supplementary table S2 Selected genes upregulated by IL-33^{ox} in ALI cultures

Function	Protein	Upregulated genes
Extracellular matrix remodelling	Serine protease	CTSC1, PCSK6
	Serine protease inhibitors	SERPINS2-10-4-1
	Metalloproteinases	ADAM8
	Cysteine protease inhibitor	CST1, FETUB
Goblet cell differentiation	Goblet cells	KLF4, SOX2, SPDEF
	Lipoxygenase	ALOX15
Carbohydrate biosynthesis machinery	Glycosyltransferase	MGAT3, ABO, ST6GAL1, ST3GAL4
	Fucosil transferases	FUT3
	Hyaluronidase	HYAL1
	Mucin glycosylation	GALNT4, GALNT6, GCNT3, B3GNT6
	Sugar metabolism	FBP1, UAP1, HS3ST1, FETUB, GNE
Components of secretory process	Mitochondrial organisation	MARK2, NDA
	ATP	ATP6V0C, EP300

	Endoplasmic reticulum/Golgi vesicle transport organisation	RAP1A
	Cellular stress	SIRT7, YBX1

Genes were selected for inclusion based on a twofold change in expression, adjusted p-value <0.05, treatment and direction.

Supplementary table S3 Fifteen cell states identified in healthy bronchial epithelial ALI cultures representing cell heterogeneity observed *in vivo* [15-19]

Cell types	Cell states	Gene marker
Basal cells	Basal	KRT5+/KRT15+/TP63+/BCAM+/COL17A1 + /KRT14+
	Basal cycling	KRT5+/MKI67+/TOP2A+/CENPF+
	Suprabasal 1	KRT5+ / KRT13+ / SERPINB4+ / KRT6A+ / SPRR1B+
	Suprabasal 2	SPRR2D+ / FN1+ / S100A8+ / SPRR1B+ /KRT16+
	Suprabasal 3	KRT4+ / SERPINB3+ / SERPINB1 + / CSTA+ / TXN+ / HES1+
Transition (Basal to differentiated cells)	Transition 1	KRT4+ (low) / SCGB3A1+ (low) /CTNNB1+ / LRRC75A+
	Transition 2	KRT4+ (low) / SCGB3A1+ (low) / HES4+ / MUC4+
Secretory cells	Club 1	CXCL5+ / CXCL6+ / LCN2+ / SAA1+ / SAA2+ / TNIP3+
	Club 2	SCGB1A1+/SCGB3A1+/BPIFA1+/BPIFB1+ /MSMB+
	Goblet	MUC5AC+/TFF3+/SPDEF+/S100P+/AQP5 +
Ciliated cells	Deuterosomal 1 (intermediate ciliated cell 1)	CDC20B+/E2F7+/PLK4+/HES6+/CCNO+

	Deuterosomal 2 (intermediate ciliated cell 2)	DEUP1+/CCNO+/SISHA8+/MUC12+/RIBC2+
	Ciliated 1	PIFO+/DNAH5+/RSPH1+/ C20orf85+/TUBA1A+/TMEM190+
Rare cell types	Ionocytes/tuft cells	CFTR+ / FOXI1+ / TMPRSS11E+ / TMEM16A+
	Neuroendocrine (pulmonary neuroendocrine cells)	ASCL1+/CALCA+/CHGA+/HOXB2+

Supplementary table S4 Gene signatures: 249 upregulated by IL-33^{ox} and 135 downregulated by inhibition of IL-33

Genes downregulated by anti-IL33 (tozorakimab) treatment in COPD ALI. NGS adjusted p-value (BH FDR) < 0.05 >2 Fold Change	Genes upregulated by IL-33^{ox} treatment in ALI NGS adjusted p-value (BH FDR) <0.05 >2 Fold Change
ITLN1	CISH
NOS2	SERPINB10
CST1	SH2D1B
CEACAM5	NEK6
PRB1	CD55
FCGBP	ITLN1
PRB2	CCL26
B3GNT6	FETUB
TSPAN8	SERPINB2

TFF3	LRRC8D
AC111149.2	CST1
SERPINB10	SLC6A14
LYZ	USP54
HMGCS2	B3GNT6
ALPL	SOCS1
FOLH1	CMYA5
ADRA2A	AC090004.2
PIK3C2G	VSIG1
GOLGA7B	ANO1
VSIG2	GALNT6
TCN1	FCGBP
HYAL1	LOXL4
FLNC	KYAT1
ST3GAL4	SLC39A8
SERPINB4	ST3GAL4
RGS13	DPP4
SLC39A8	MCUB
DEFB1	KCNK6
CSTA	EPS8L1
SLC6A14	STN1
LCN2	NOS2
CD36	ARHGAP40
S100P	CEACAM5
CTSC	SPDEF
SH2D6	CYP27B1

ATOH8	GALNT4
RNASE1	GGH
DPP4	ALOX15
SH2D1B	AL121761.1
SFTPA2	CTSC
TRABD2A	HS3ST1
KCNE3	NPDC1
CST4	LRRC31
PYCR1	GADD45G
AL163636.2	CEACAM21
EPHX4	SEC14L1
TRPV6	CD9
HKDC1	PLS1
HGD	SLC25A1
LGALS7	GNE
SLC5A8	TSPAN3
AZGP1	CDH26
KRT23	LINC01995
TNFRSF13C	BCL2L15
VSIG1	FUT3
CD55	CYTIP
TIMP1	DOK1
FOXA3	ATP12A
CHRM1	RAP1GAP
MMP28	LINC01269
SLC7A11	INSIG1

GPSM3	SIRT7
FAM177B	KCNE3
SERPINB11	CAPN14
HVCN1	NOP53
FA2H	PPP4R1L
HBEGF	SERPINB4
SERPINA11	SUSD2
AP002498.1	KLF4
GPX2	TMC1
TINAGL1	GCNT3
PTPRN2	RPL7L1P8
KDELR3	PSTPIP1
KIF21B	OTOGL
RPTN	PARD3B
ADM2	ITPRID2
PDE8B	TRABD2A
RHOH	TRPV6
SLC26A4-AS1	ATOH8
GCNT3	DGKA
AC090004.2	ERVH-1
TRPM5	CAMK1D
GNG13	SLC12A2
BCL2L15	ADRA2A
CHAD	AL353807.5
FXYD6	HES4
SLURP2	AMN

SH2D7	AC007255.1
ANO1	AP000547.3
CHAT	TMPRSS2
CYTIP	UAP1
AL121761.1	PRB2
CA2	TLR4
SLC26A4	SLC9B2
MZB1	LGALS4
TAS1R3	MGAT3
RCAN1	ELOVL5
CLDN22	VWF
UGT2A1	FA2H
IGSF22	PRR15
TMEM139	ST6GAL1
CST2	CHCHD10
CISH	DHX32
LRRC31	HPGD
GADD45G	DUOX2
SPDEF	LINC01994
DOK1	NFE2
TMEM211	ALPL
BDNF	SLAMF6P1
APOE	TNIK
ARHGAP40	H1-10
MPEG1	SULF1
GAREM2	SERPINB11

ATP13A5	TSPAN13
FMOD	AP001372.3
RIMS3	AC021055.1
MSMB	TMUB1
BMX	TMEM92
PSTPIP1	GDNF
TFF1	KANK3
GDNF	ALKAL1
SEPTIN9-DT	AL353807.3
OR2I1P	TMEM139
NFE2	HPDL
SELP	PHETA2
NTAN1	LINC00896
C2CD4A	MFSD4A
NCF1C	NAPRT
ANO7	DPP4-DT
RIMKLA	RETREG1
CCL22	SLC7A1
CDH19	CLLU1-AS1
BX640514.2	CREB3L1
TMC1	DQX1
SH3PXD2A-AS1	TMEM71
	ZNF467
	CD274
	FOLH1
	S100P

	CYP2C9
	LBH
	HYAL1
	APOL4
	FGF13
	COLCA1
	ATP13A5
	HPCAL1
	SOX2
	KDELR3
	NUDT8
	CA2
	PACSIN1
	FAM177B
	ADAMTS9
	DAB2
	CNKSR3
	MAFF
	ORAI1
	AL358777.3
	ABCG2
	CLDN5
	SLC7A4
	AC020656.1
	PPP1R1B
	SIGLEC16

	KIF1C
	AL163636.2
	SRARP
	ZNF579
	FER1L6
	SHISA8
	A4GALT
	LINC00866
	TYMP
	SCIN
	FLNC
	FZD5
	TENM2
	ANKRD9
	AC006059.2
	ADAM8
	SLC27A3
	CCDC85B
	PLA2G3
	AL583836.1
	NTRK2
	PYCR1
	CD36
	ANXA6
	KCNJ16
	TMEM178A

	OIT3
	NR4A1
	LINC01504
	RHOH
	FGF12
	CREB3L4
	SLC26A4-AS1
	SULT1C2
	NPSR1
	POU2AF1
	C1QTNF1
	AP002498.1
	ADCY4
	PKHD1L1
	PCSK6
	ABO
	ZNF205
	FLT1
	AADAC
	LYZ
	MYO1A
	TREML2
	AC246817.1
	ADM5
	SERPINB13
	TAT

	ABHD17A
	ARMC10
	ANG
	FAM3B
	LINP1
	LY75-CD302
	AC023024.1
	AHSG
	LDHD
	POSTN
	AL139317.3
	ITGA10
	EPS8L3
	SIDT1
	FBP1
	CYP1B1-AS1
	SLC29A4
	IL1RL2
	ARHGEF35-AS1
	SLC5A5
	SNORC
	TRIM7
	ADM2
	GTF2IRD2B
	KCND2
	VSIG2

	CERS1
	KAZALD1
	ZNF442
	CYP2G2P
	ANTKMT
	AL441992.3

ALI: air–liquid interface; BH: Benjamini–Hochberg; COPD: chronic obstructive pulmonary disease; FDR: false discovery rate; NGS: next-generation sequencing.

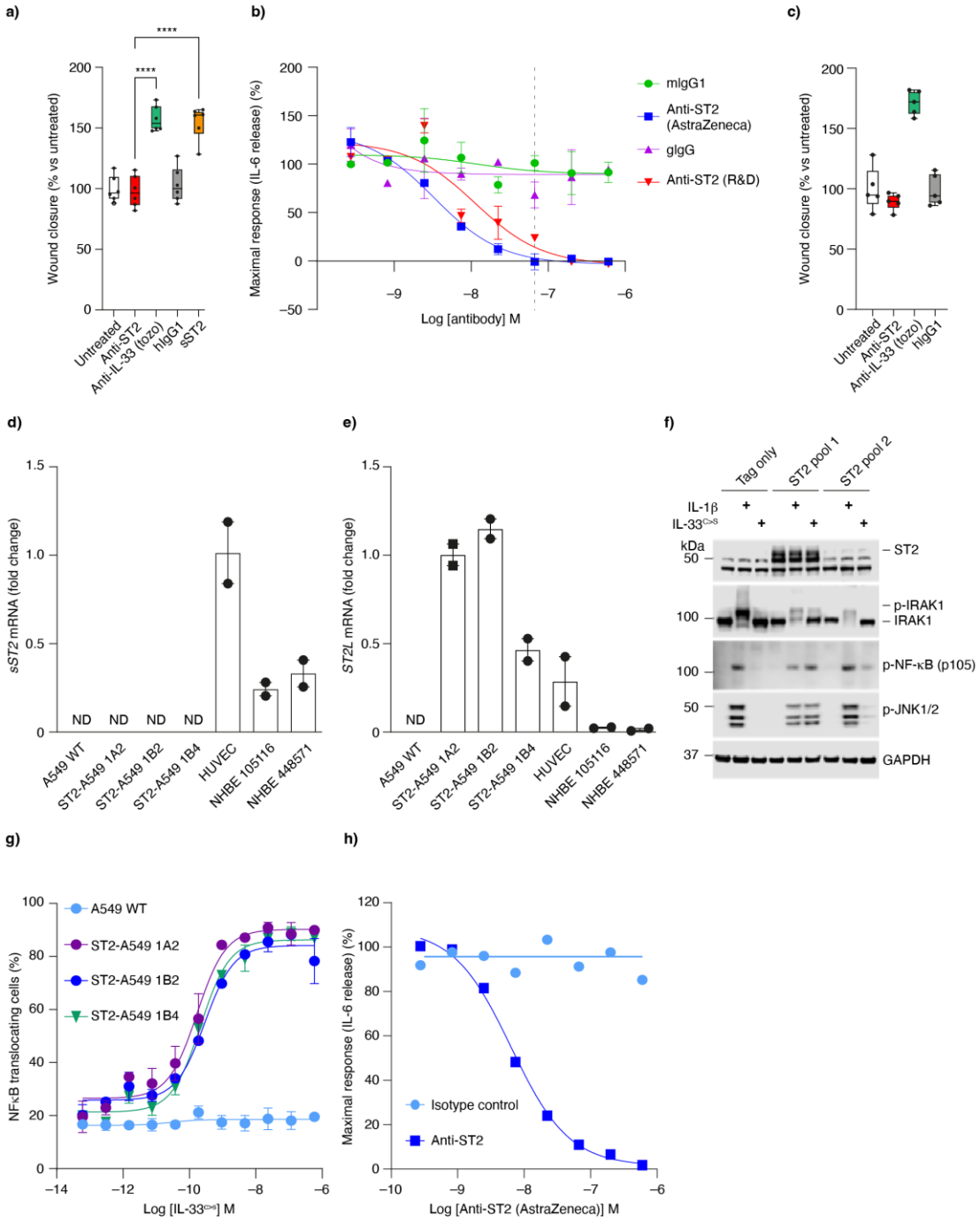
a)
Wound closure (% vs untreated)
Untreated
Anti-ST2
Anti-IL-33 (tozo)
hIgG1
sST2
b)
Maximal response (IL-6 release) (%)
Log [antibody] M
mIgG1
Anti-ST2 (AstraZeneca)
gIgG
Anti-ST2 (R&D)
c)
Wound closure (% vs untreated)
d)
sST2 mRNA (fold change)
ND
A549 WT
ST2-A549 1A2
ST2-A549 1B2
ST2-A549 1B4
HUVEC
NHBE 105116
NHBE 448571
e)
ST2L mRNA (fold change)
f)
Tag only
ST2 pool 1
ST2 pool 2
IL-1β
IL-33C>S
kDa
ST2
p-IRAK1
IRAK1
p-NF-κB (p105)
p-JNK1/2
GAPDH
g)
NFκB translocating cells (%)
Log [IL-33C>S] M
h)
Maximal response (IL-6 release) (%)
Isotype control
Anti-ST2
Log [Anti-ST2 (AstraZeneca)] M

Supplementary figure S1 IL-33^{ox}-mediated response is independent of the ST2 receptor

a) Scratch wound closure in growth factor starved submerged NHBE cells at 24 h following treatment with ST2-neutralising antibody (goat), IL-33-neutralising antibody (tozorakimab), hIgG1 isotype control antibody or sST2, versus untreated control (five individual donors). b) IL-6 release in HUVECs following 30 min pre-treatment with a titration of ST2-neutralising antibodies or isotype control antibodies, followed by 20 h stimulation with IL-33$^{C>S}$ (two replicate wells per condition). Vertical dotted line indicates the concentration of anti-ST2 antibody (AstraZeneca) required to achieve complete suppression of IL-6 release, used in figure 1a. c) Scratch wound closure in FCS-starved A549 cells at 24 h following treatment with ST2-neutralising antibody (goat), tozorakimab or hIgG1 isotype control antibody, versus untreated control (data points show individual wells). d) RT-qPCR of sST2 in A549 cells, A549 transduced with ST2 (clones 1A2, 1B2, 1B4), HUVECs and NHBE cells; data are normalised to HUVECs e) RT-qPCR of membrane-associated ST2 in A549 cells, A549 transduced with ST2, HUVECs and NHBE cells; data are normalised to A549 cells transduced with ST2. f) Western blot analysis of ST2, IRAK1, p-NF-κB and p-JNK1/2 in A549 epithelial cells transduced with tag alone or tagged ST2 cDNA (two pools of cells), stimulated with IL-1β or IL-33$^{C>S}$ for 10 min (GAPDH as a loading control). g) NF-κB translocation from the cytoplasm to the nucleus in A549 cells or clones (1A2, 1B2, 1B4) stably expressing ST2 following treatment with IL-33$^{C>S}$. h) IL-6 release in A549 ST2 clone 1A2 pre-incubated with ST2-neutralising or isotype control antibodies, followed by treatment for 20 h with IL-33$^{C>S}$. In panels a and c, box plots display median with single data points shown; data are normalised to untreated control. Further details on box plots and statistical analysis can be found in the supplementary materials and methods. ****p≤0.0001. In panels b and h, data are plotted as % of maximal response, where 20 h with IL-33$^{C>S}$ in the absence of any antibody is considered 100% response;

data plotted as mean of duplicates±SEM. In panels d and e, data are plotted as mean±SEM. ND: not detected.

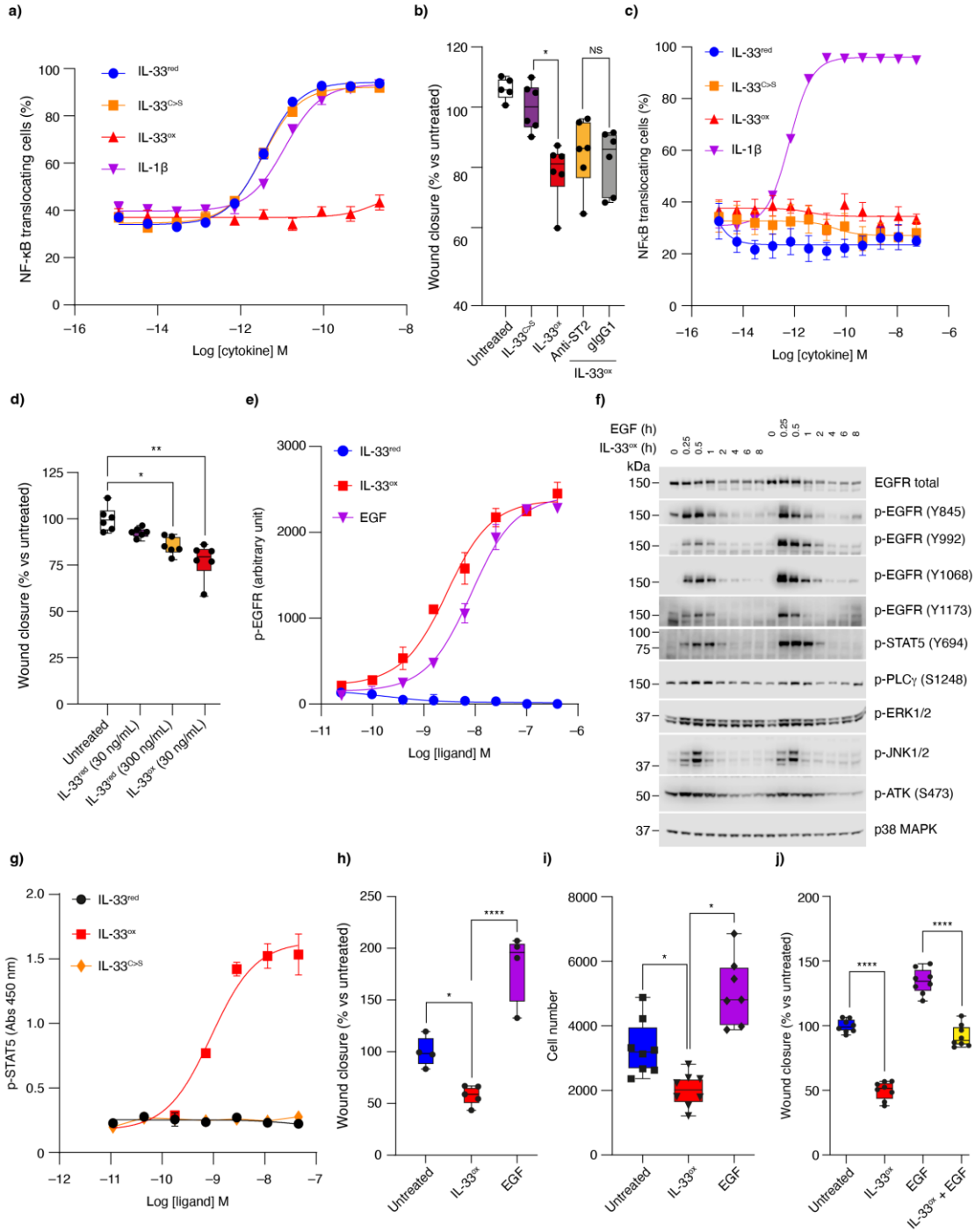
a)
b)
c)
NF-κB translocating cells (%)
Log [cytokine] M
IL-33red
IL-33C>S
IL-33ox
IL-1β
Wound closure (% vs untreated)
Untreated
Anti-ST2
gIgG1
NS
NFκB translocating cells (%)
d)
e)
f)
Wound closure (% vs untreated)
IL-33red (30 ng/mL)
IL-33red (300 ng/mL)
IL-33ox (30 ng/mL)
p-EGFR (arbitrary unit)
Log [ligand] M
EGF
EGF (h)
kDa
EGFR total
p-EGFR (Y845)
p-EGFR (Y992)
p-EGFR (Y1068)
p-EGFR (Y1173)
p-STAT5 (Y694)
p-PLCγ (S1248)
p-ERK1/2
p-JNK1/2
p-ATK (S473)
p38 MAPK
g)
h)
i)
j)
p-STAT5 (Abs 450 nm)
Cell number
EGF
IL-33ox + EGF

Supplementary figure S2 IL-33^{ox} impairs wound closure via EGFR signalling

a) NF-κB translocation from the cytoplasm to the nucleus in ST2-expressing HUVECs following 30 min treatment with a titration of IL-33^{red}, IL-33$^{C>S}$, IL-33^{ox} or IL-1β (two wells per data point). b) Scratch wound closure of A549 cells at 24 h following treatment with IL-33$^{C>S}$, IL-33^{ox}, IL-33^{ox} + ST2-neutralising antibody or IL-33^{ox} + gIgG1 isotype control antibody, versus untreated control. Data points show replicates; data are normalised to one replicate in the untreated control group. c) NF-κB translocation from the cytoplasm to the nucleus in A549 cells following 30 min treatment with a titration of IL-33^{red}, IL-33$^{C>S}$, IL-33^{ox} or IL-1β (two wells per data point). d) Scratch wound closure at 24 h following treatment with increasing concentrations of IL-33^{red} or IL-33^{ox} versus untreated control in NHBE cells from healthy donors (six individual donors). e) HTRF measurement of p-EGFR following a 15 min titration of IL-33^{red}, IL-33^{ox} or EGF in NHBE cells (two wells per data point); arbitrary units. f) Western blot analysis of total EGFR, p-EGFR and key signalling molecules downstream of EGFR over time in A549 cells treated with EGF or IL-33^{ox}. g) ELISA measurement of p-STAT5 following a 30 min titration of IL-33^{red}, IL-33^{ox} or IL-33$^{C>S}$ in A549 cells (two wells per data point); absorption at 450 nm shown. h) Scratch wound closure in NHBE cells at 24 h following treatment with IL-33^{ox} or EGF, versus untreated control (four to five individual donors). i) Proliferation of A549 cells at 24 h following treatment with IL-33^{ox} or EGF, or untreated control. Data points show replicates. j) Scratch wound closure in A549 cells at 24 h following treatment with IL-33^{ox}, EGF or IL-33^{ox} + EGF, versus untreated control. Data points show replicates. In panels a, c and g, error bars show SEM. Individual data points are shown in panels c, h, i and j, and further details of box plots and statistics can be found in the supplementary materials and methods. *p≤0.05; **p≤0.01; ****p≤0.0001, NS: not significant.

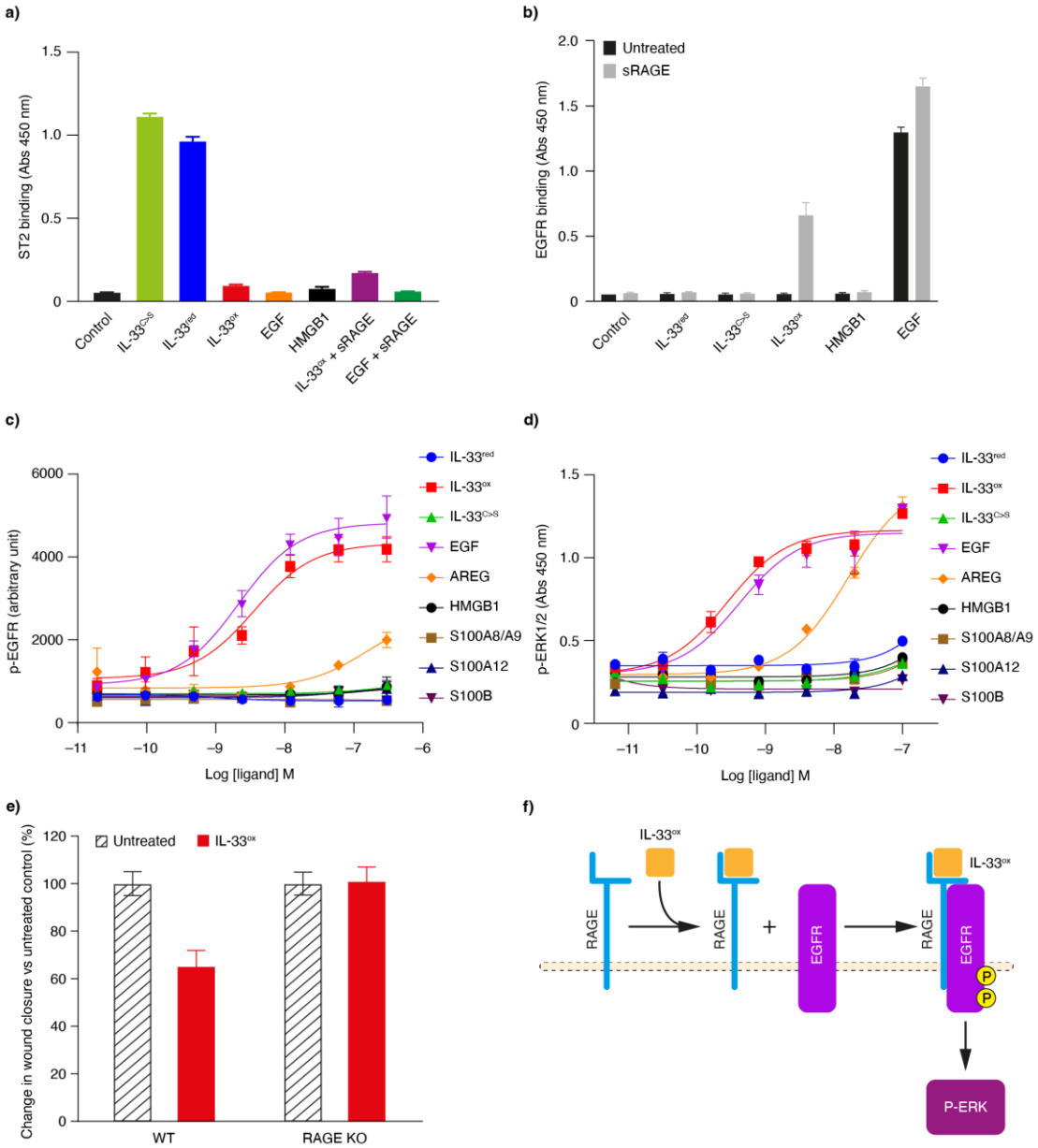
a)
ST2 binding (Abs 450 nm)
Control
IL-33C>S
IL-33red
IL-33ox
EGF
HMGB1
IL-33ox + sRAGE
EGF + sRAGE
b)
Untreated
sRAGE
EGFR binding (Abs 450 nm)
c)
p-EGFR (arbitrary unit)
Log [ligand] M
IL-33red
IL-33ox
IL-33C>S
EGF
AREG
HMGB1
S100A8/A9
S100A12
S100B
d)
p-ERK1/2 (Abs 450 nm)
e)
Change in wound closure vs untreated control (%)
WT
RAGE KO
f)
RAGE
EGFR
P-ERK

Supplementary figure S3 Comparison of EGFR and RAGE ligands with IL-33^{ox}

a) Direct ELISA detecting binding of ST2-Fc to immobilised nonspecific control protein, IL-33$^{C>S}$, IL-33^{red}, IL-33^{ox}, EGF or HMGB1 in the presence or absence of soluble RAGE. b) Direct MUC5AC detecting binding of EGFR-Fc to immobilised IL-33^{red}, IL-33$^{C>S}$, IL-33^{ox}, HMGB1 or EGF in the presence or absence of soluble RAGE. c) HTRF analysis of p-EGFR levels in A549 cells stimulated with a titration of IL-33^{red}, IL-33^{ox}, IL-33$^{C>S}$, EGF, AREG, HMGB1, S100A8/A9, S100A12 or S100B for 15 min (average of three independent experiments). d) ELISA analysis of p-ERK1/2 levels in A549 cells stimulated with a titration of IL-33^{red}, IL-33^{ox}, IL-33$^{C>S}$, EGF, AREG, HMGB1, S100A8/A9, S100A12 or S100B for 15 min (average of three independent experiments). e) Change in scratch wound closure of A549 cells or RAGE KO A549 cells at 24 h following treatment with IL-33^{ox} versus untreated control (data averaged from 12 wells). f) Schematic representation of IL-33^{ox}, RAGE and EGFR protein complex. In panels a–e, error bars show SEM.

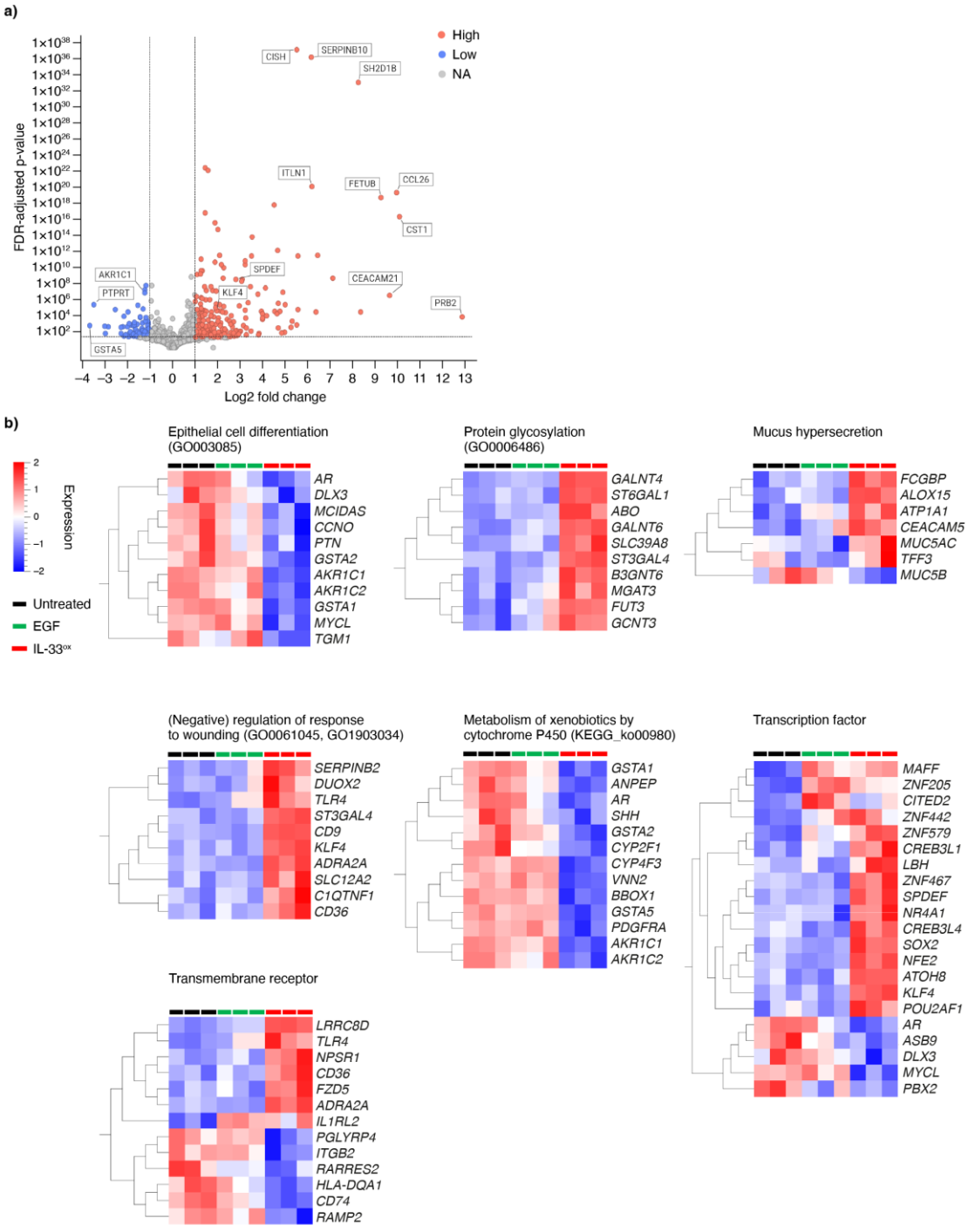
a)
High
Low
NA
FDR-adjusted p-value
Log2 fold change
CISH
SERPINB10
SH2D1B
ITLN1
FETUB
CCL26
CST1
SPDEF
CEACAM21
PRB2
KLF4
AKR1C1
PTPRT
GSTA5
b)
Expression
Untreated
EGF
IL-33ox
Epithelial cell differentiation (GO003085)
AR
DLX3
MCIDAS
CCNO
PTN
GSTA2
AKR1C1
AKR1C2
GSTA1
MYCL
TGM1
Protein glycosylation (GO0006486)
GALNT4
ST6GAL1
ABO
GALNT6
SLC39A8
ST3GAL4
B3GNT6
MGAT3
FUT3
GCNT3
Mucus hypersecretion
FCGBP
ALOX15
ATP1A1
CEACAM5
MUC5AC
TFF3
MUC5B
(Negative) regulation of response to wounding (GO0061045, GO1903034)
SERPINB2
DUOX2
TLR4
ST3GAL4
CD9
KLF4
ADRA2A
SLC12A2
C1QTNF1
CD36
Metabolism of xenobiotics by cytochrome P450 (KEGG_ko00980)
GSTA1
ANPEP
AR
SHH
GSTA2
CYP2F1
CYP4F3
VNN2
BBOX1
GSTA5
PDGFRA
AKR1C1
AKR1C2
Transcription factor
MAFF
ZNF205
CITED2
ZNF442
ZNF579
CREB3L1
LBH
ZNF467
SPDEF
NR4A1
CREB3L4
SOX2
NFE2
ATOH8
KLF4
POU2AF1
AR
ASB9
DLX3
MYCL
PBX2
Transmembrane receptor
LRRC8D
TLR4
NPSR1
CD36
FZD5
ADRA2A
IL1RL2
PGLYRP4
ITGB2
RARRES2
HLA-DQA1
CD74
RAMP2

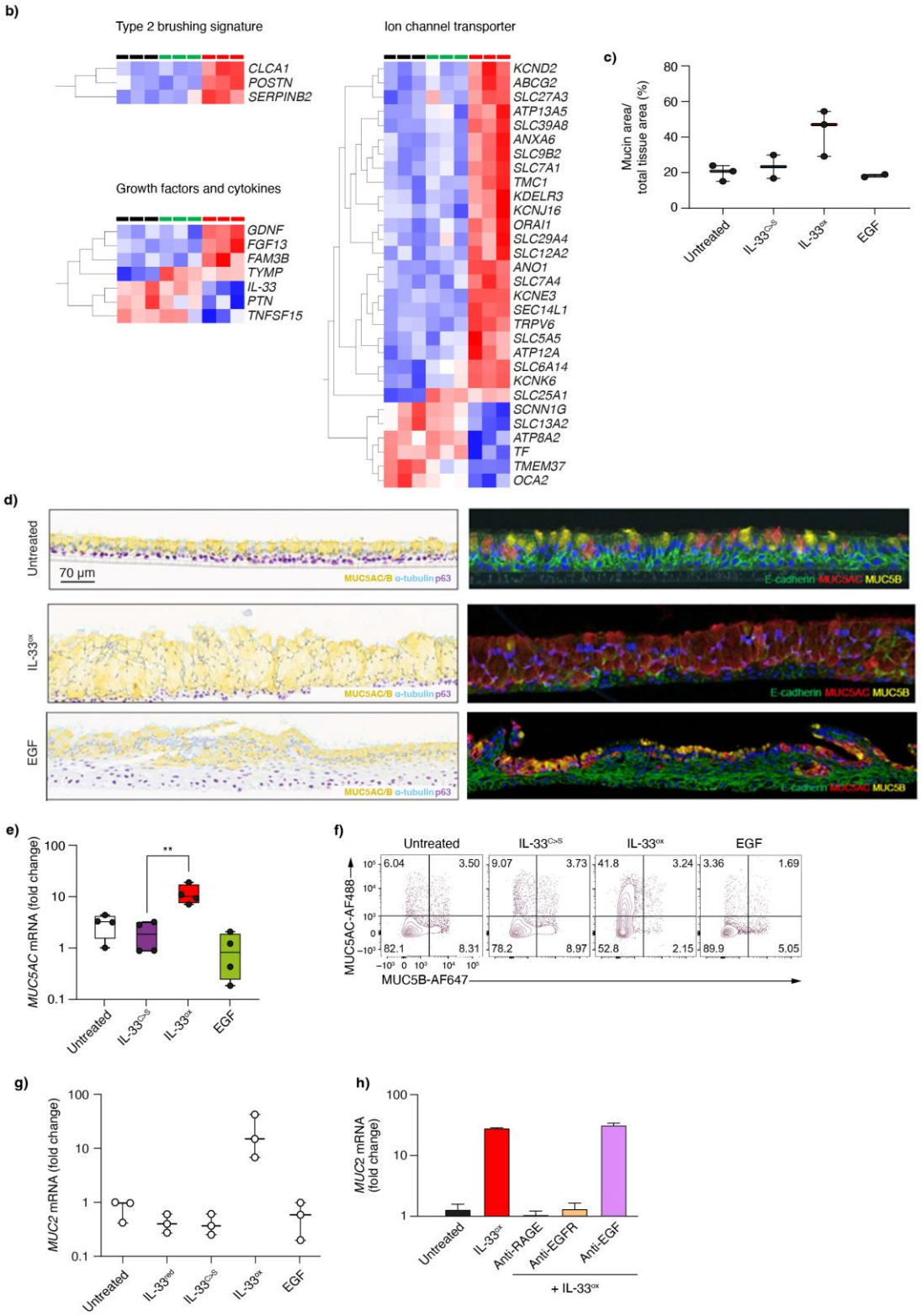
b)
Type 2 brushing signature
CLCA1
POSTN
SERPINB2
Growth factors and cytokines
GDNF
FGF13
FAM3B
TYMP
IL-33
PTN
TNFSF15
Ion channel transporter
KCND2
ABCG2
SLC27A3
ATP13A5
SLC39A8
ANXA6
SLC9B2
SLC7A1
TMC1
KDELR3
KCNJ16
ORAI1
SLC29A4
SLC12A2
ANO1
SLC7A4
KCNE3
SEC14L1
TRPV6
SLC5A5
ATP12A
SLC6A14
KCNK6
SLC25A1
SCNN1G
SLC13A2
ATP8A2
TF
TMEM37
OCA2
c)
Mucin area/ total tissue area (%)
Untreated
IL-33C>S
IL-33ox
EGF
d)
Untreated
IL-33ox
EGF
70 µm
MUC5AC/B α-tubulin p63
E-cadherin MUC5AC MUC5B
e)
MUC5AC mRNA (fold change)
**
Untreated
IL-33C>S
IL-33ox
EGF
f)
Untreated
IL-33C>S
IL-33ox
EGF
MUC5AC-AF488
MUC5B-AF647
6.04
3.50
82.1
8.31
9.07
3.73
78.2
8.97
41.8
3.24
52.8
2.15
3.36
1.69
89.9
5.05
g)
MUC2 mRNA (fold change)
Untreated
IL-33red
IL-33C>S
IL-33ox
EGF
h)
MUC2 mRNA (fold change)
Untreated
IL-33ox
Anti-RAGE
Anti-EGFR
Anti-EGF
+ IL-33ox

Supplementary figure S4 IL-33^{ox} induces transcriptional changes in bronchial epithelial ALI cultures as shown by bulk RNA analysis

a) Volcano plot representing differential expression of genes from bulk RNA sequencing in ALI cultures treated with IL-33^{ox} versus untreated control. b) Heat maps showing changes in gene expression levels by gene families in bronchial ALI cultures following treatment with IL-33^{ox} or EGF, or untreated control (three individual donors). c) Quantification of mucin area from healthy donors treated with IL-33$^{C>S}$, IL-33^{ox} or EGF, or untreated control (two–three individual donors). d) Left panels, immunohistochemistry of healthy ALI cultures following treatment with IL-33^{ox} or EGF, or untreated control. MUC5AC/B for goblet cells (yellow), acetylated α-tubulin for ciliated cells (teal) and p63 for basal cells (purple). Right panels, immunofluorescence showing changes in MUC5AC (red), MUC5B (yellow) and tight junction (E-cadherin, green) levels in healthy ALI cultures or following treatment with IL-33^{ox} or EGF, or untreated control (scale bar=70 µm). e) *MUC5AC* expression determined by RT-qPCR in healthy bronchial ALI cultures treated with 30 ng/mL of IL-33$^{C>S}$, IL-33^{ox} or EGF, or untreated control for 7 days; for all conditions, media was changed every three days on the basal side of the ALI culture. Single data points from four individual donors shown; data are normalised to one donor in the untreated control group. f) Flow cytometry analysis of intracellular MUC5AC or MUC5B in dissociated bronchial ALI cultures following treatment with IL-33$^{C>S}$, IL-33^{ox} or EGF, or untreated control (seven individual donors). g) *MUC2* expression determined by RT-qPCR in ALI cultures following treatment with IL-33^{red}, IL-33$^{C>S}$, IL-33^{ox} or EGF, or untreated control (three individual donors). Single data points from individual donors are shown; data are normalised to one donor in the untreated healthy control group. h) *MUC2* expression determined by RT-qPCR in ALI cultures following treatment with IL-33^{ox} or IL-33^{ox} + RAGE-neutralising, EGFR-neutralising or EGF-neutralising antibodies, or untreated control (two individual donors). In panels g and h, error bars

show SEM. Individual data points are shown in panels c, and e, and further details of box plots can be found in the supplementary materials and methods. **p≤0.01.

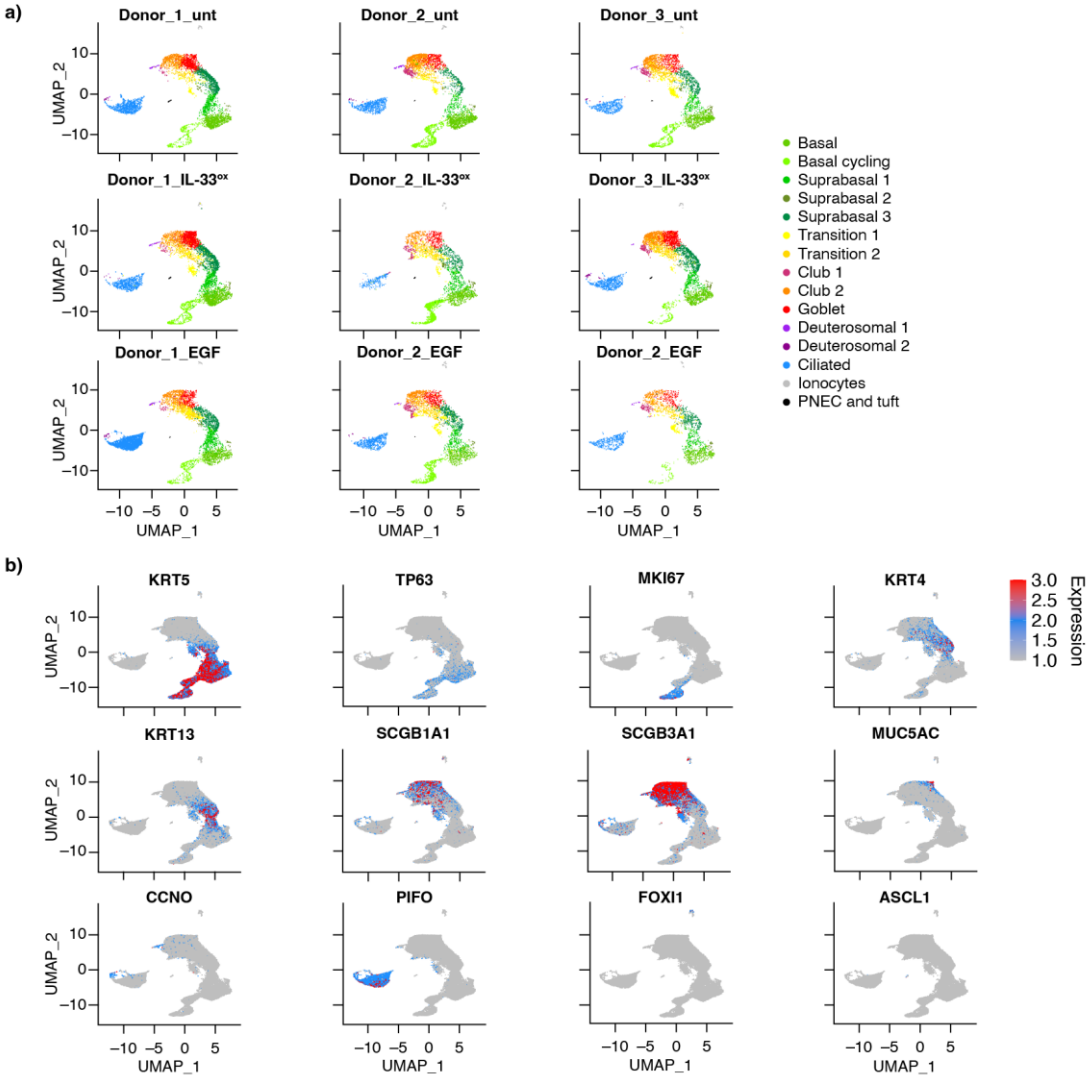
a)
Donor_1_unt
Donor_2_unt
Donor_3_unt
Donor_1_IL-33ox
Donor_2_IL-33ox
Donor_3_IL-33ox
Donor_1_EGF
Donor_2_EGF
Donor_2_EGF
UMAP_1
UMAP_2
Basal
Basal cycling
Suprabasal 1
Suprabasal 2
Suprabasal 3
Transition 1
Transition 2
Club 1
Club 2
Goblet
Deuterosomal 1
Deuterosomal 2
Ciliated
Ionocytes
PNEC and tuft
b)
KRT5
TP63
MKI67
KRT4
KRT13
SCGB1A1
SCGB3A1
MUC5AC
CCNO
PIFO
FOXI1
ASCL1
Expression
c)
Basal
Basal cycling
Suprabasal 1
Suprabasal 2
Suprabasal 3
Transition 1
Transition 2
Club 1
Club 2
Goblet
Deuterosomal 1
Deuterosomal 2
Ciliated
Ionocytes
PNEC and tuft
KRT5
TP63
KRT14
DLK2
BCAM
MKI67
STMN1
TOP2A
FABP5
KRT13
KRT4
KRT19
SERPINB4
HES4
NOTCH3
SCGB1A1
SCGB3A1
MSMB
CYP2F1
TMEM45A
CEACAM5
MUC5AC
SPDEF
FOXA3
TFF3
DEUP1
CCNO
FOXJ1
PIFO
IFT57
LRRC23
TSPAN19
DNAH5
FOXI1
CFTR
ASCL1
POU2F3
RGS13
Expression

Supplementary figure S5 Single-cell transcriptomic confirmation of airway epithelial cell state in healthy bronchial epithelial ALI cultures

a) UMAP plots of healthy ALI cultures treated for 7 days with IL-33^{ox} (n=3; 15 231 cells), EGF (n=3; 12 943 cells), or untreated control (n=3; 14 976 cells), displaying the annotated cell states/types. b) UMAP plots of healthy untreated ALI cultures depicting known cell markers for distinguished cell states in the airway epithelium. c) Heat map showing average expression levels of key genes used for cell state identification in healthy untreated ALI cultures.

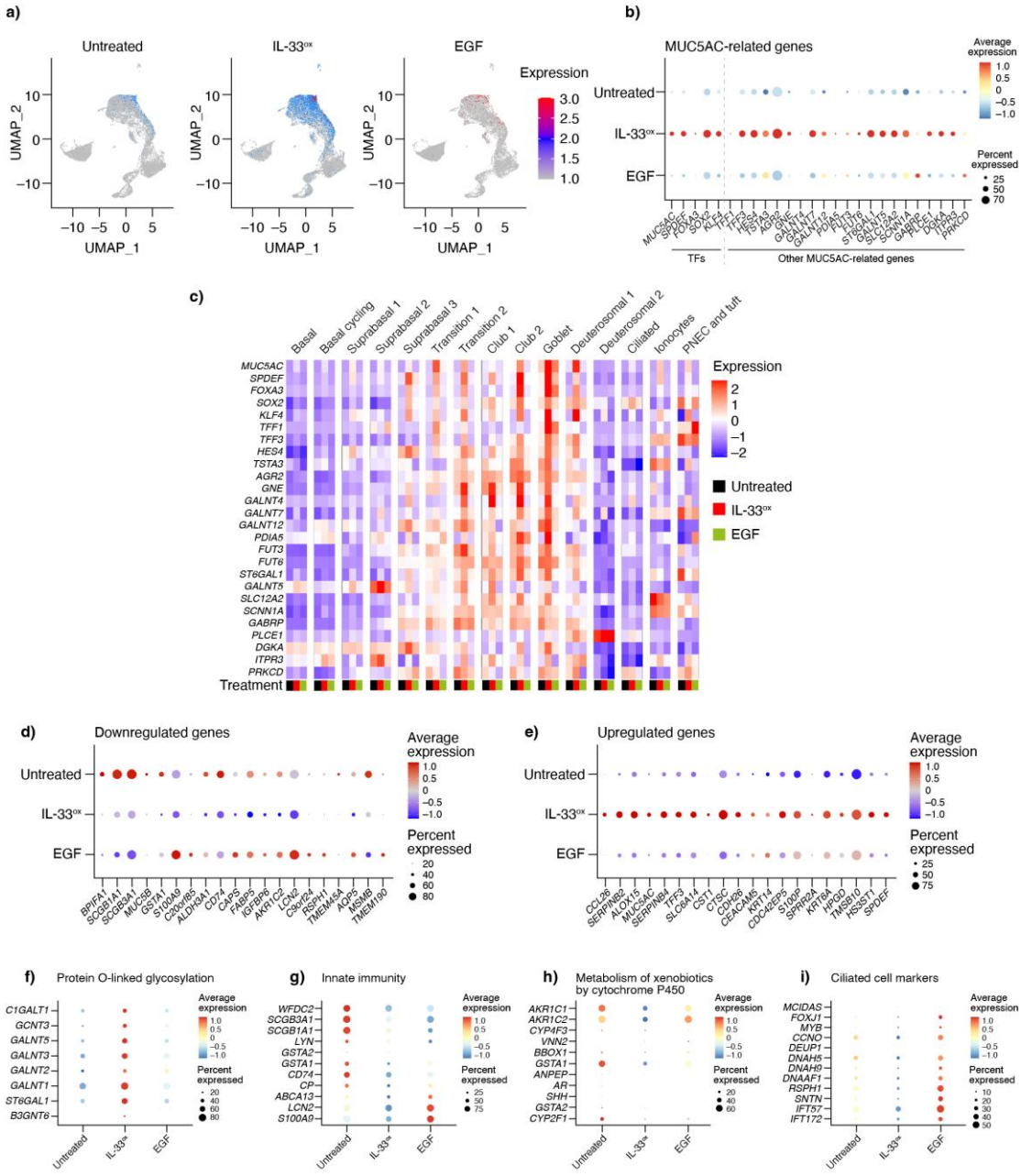
a)
Untreated
IL-33ox
EGF
UMAP_2
UMAP_1
Expression
b)
MUC5AC-related genes
Untreated
IL-33ox
EGF
Average expression
Percent expressed
TFs
Other MUC5AC-related genes
c)
Basal
Basal cycling
Suprabasal 1
Suprabasal 2
Suprabasal 3
Transition 1
Transition 2
Club 1
Club 2
Goblet
Deuterosomal 1
Deuterosomal 2
Ciliated
Ionocytes
PNEC and tuft
Expression
Untreated
IL-33ox
EGF
Treatment
d)
Downregulated genes
e)
Upregulated genes
f)
Protein O-linked glycosylation
g)
Innate immunity
h)
Metabolism of xenobiotics by cytochrome P450
i)
Ciliated cell markers

Supplementary figure S6 IL-33^{ox} induces transcriptional changes in bronchial epithelial ALI cultures as shown by single-cell transcriptomics

a) UMAP plots showing SPDEF-expressing cells in ALI cultures after treatment with IL-33^{ox} or EGF, versus untreated control. b) Dot plot showing the expression levels of MUC5AC-related genes in ALI cultures treated with IL-33^{ox} or EGF, or untreated control. c) Heat map showing changes in gene expression levels measured by single-cell RNA analysis in ALI cultures in the annotated cell states/types following treatment with IL-33^{ox} or EGF, or untreated control. d) Dot plot showing the most significantly downregulated genes in ALI cultures treated with IL-33^{ox} or EGF, in comparison with untreated control, considering all cell states/types (Wilcoxon rank sum test, $p \leq 0.001$). e) Dot plot showing the most significantly upregulated genes in ALI cultures treated with IL-33^{ox} or EGF, in comparison with untreated control, considering all cell states/types (Wilcoxon rank sum test, $p \leq 0.001$). f–i) Dot plots showing average expressions of genes involved in (f) protein glycosylation, (g) innate immunity, (h) P450 metabolism and (i) ciliated cell markers in healthy ALI cultures following treatment with IL-33^{ox} or EGF, versus untreated controls. In panels b and d–i, the size of the dot represents the percentage of cells expressing the gene. TF: transcription factor.

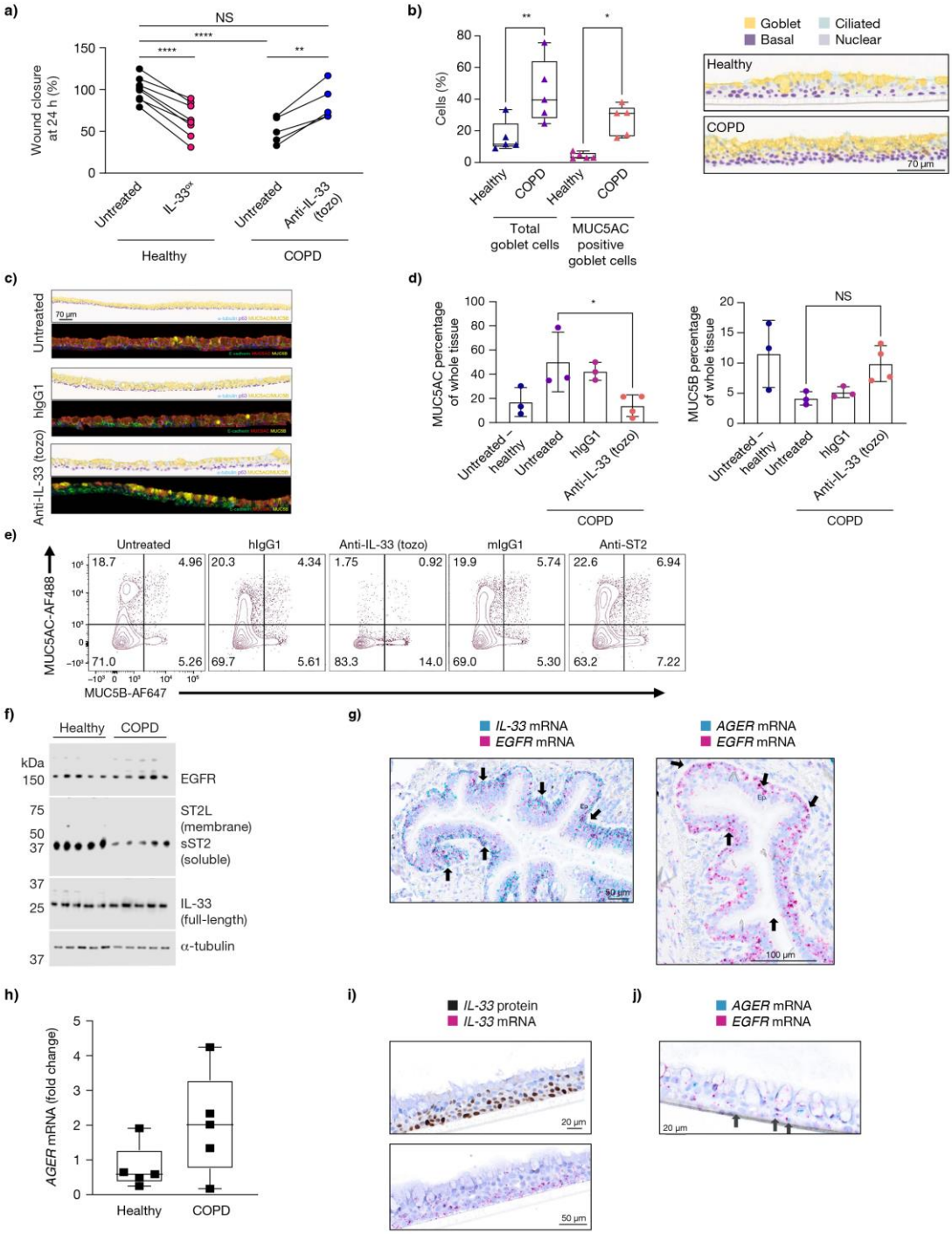
a)
NS
****
****
**
Wound closure at 24 h (%)
150
100
50
0
Untreated
IL-33ext
Untreated
Anti-IL-33 (tozo)
Healthy
COPD
b)
**
*
Cells (%)
80
60
40
20
0
Healthy
COPD
Healthy
COPD
Total goblet cells
MUC5AC positive goblet cells
Goblet
Ciliated
Basal
Nuclear
Healthy
COPD
70 µm
c)
Untreated
hIgG1
Anti-IL-33 (tozo)
70 µm
d)
MUC5AC percentage of whole tissue
100
80
60
40
20
0
*
Untreated – healthy
Untreated
hIgG1
Anti-IL-33 (tozo)
COPD
MUC5B percentage of whole tissue
20
15
10
5
0
NS
Untreated – healthy
Untreated
hIgG1
Anti-IL-33 (tozo)
COPD
e)
Untreated
hIgG1
Anti-IL-33 (tozo)
mIgG1
Anti-ST2
MUC5AC-AF488
MUC5B-AF647
18.7
4.96
71.0
5.26
20.3
4.34
69.7
5.61
1.75
0.92
83.3
14.0
19.9
5.74
69.0
5.30
22.6
6.94
63.2
7.22
f)
Healthy
COPD
kDa
150
EGFR
75
50
37
ST2L (membrane)
sST2 (soluble)
37
25
IL-33 (full-length)
37
α-tubulin
g)
IL-33 mRNA
EGFR mRNA
AGER mRNA
EGFR mRNA
50 µm
100 µm
h)
AGER mRNA (fold change)
5
4
3
2
1
0
Healthy
COPD
i)
IL-33 protein
IL-33 mRNA
20 µm
50 µm
j)
AGER mRNA
EGFR mRNA
20 µm

Supplementary figure S7 The IL-33^{ox}–RAGE/EGFR pathway is active in bronchial epithelial COPD ALI cultures and mediates mucin production

a) Paired scratch wound closure in healthy human bronchial epithelial cells treated with IL-33^{ox} or untreated control, and in COPD-diseased human bronchial epithelial cells treated with IL-33 neutralising antibody (tozorakimab) or untreated control (eight individual heathy donors, four individual COPD donors). b) Flow cytometry analysis (left) and immunohistochemistry (right) showing changes in goblet cell levels in healthy ALI cultures compared with COPD ALI cultures (scale bar=70 µm) (five individual heathy donors, five individual COPD donors). c) Immunohistochemistry (top) of COPD ALI cultures treated with tozorakimab or hIgG1 isotype control antibody, or untreated control. MUC5AC/B for goblet cells (yellow), acetylated α-tubulin for ciliated cells (teal) and p63 for basal cells (purple). Immunofluorescence (bottom) showing changes in MUC5AC (red), MUC5B (yellow) and tight junctions (E-cadherin, green) in COPD ALI cultures treated with tozorakimab or hIgG1 isotype control antibody, or untreated control (scale bar=70 µm). d) Quantification of immunofluorescence showing increased MUC5AC-positive goblet cells in untreated COPD ALI cultures compared with healthy ALI cultures, and in COPD ALI cultures treated with hIgG1 isotype control antibody or tozorakimab (three individual heathy donors, three-four individual COPD donors). e) Flow cytometry analysis of intracellular MUC5AC and MUC5B in COPD ALI cultures treated with tozorakimab, ST2-neutralising or the relevant isotype control antibodies, or untreated control. f) Western blot analysis of EGFR, ST2L, sST2 and IL-33 levels in ALI cultures generated from healthy (five individual donors) and COPD (five individual donors) donors (α-tubulin as a loading control). g) Simultaneous visualisation of small airway *EGFR* and *IL-33* mRNA (left, scale bar=50 µm) and *AGER* (gene encoding RAGE protein) and *EGFR* mRNA (right, scale bar=100 µm) by double chromogenic *in situ* hybridisation of lung sections from patients with COPD. h) *AGER* expression determined by RT-qPCR in healthy (five individual donors) or COPD (five

individual donors) ALI cultures. i) Immunohistochemistry (top) of IL-33 protein (scale bar=20 µm) and *in situ* hybridisation detection (bottom) of *IL-33* mRNA in COPD ALI cultures (scale bar=50 µm). j) Double *in situ* hybridisation detection of *AGER* and *EGFR* mRNA in COPD ALI cultures (scale bar=20 µm). In panels b, d and h, error bars show SEM. *p≤0.05; **p≤0.01; ****p≤0.0001. In panels b, d, and h, single data points from individual donors are shown; data are normalised to one donor in the healthy untreated control group. In panels g and j, arrows show representative cells double positive for the indicated mRNA. EP: epithelium; NS: not significant.

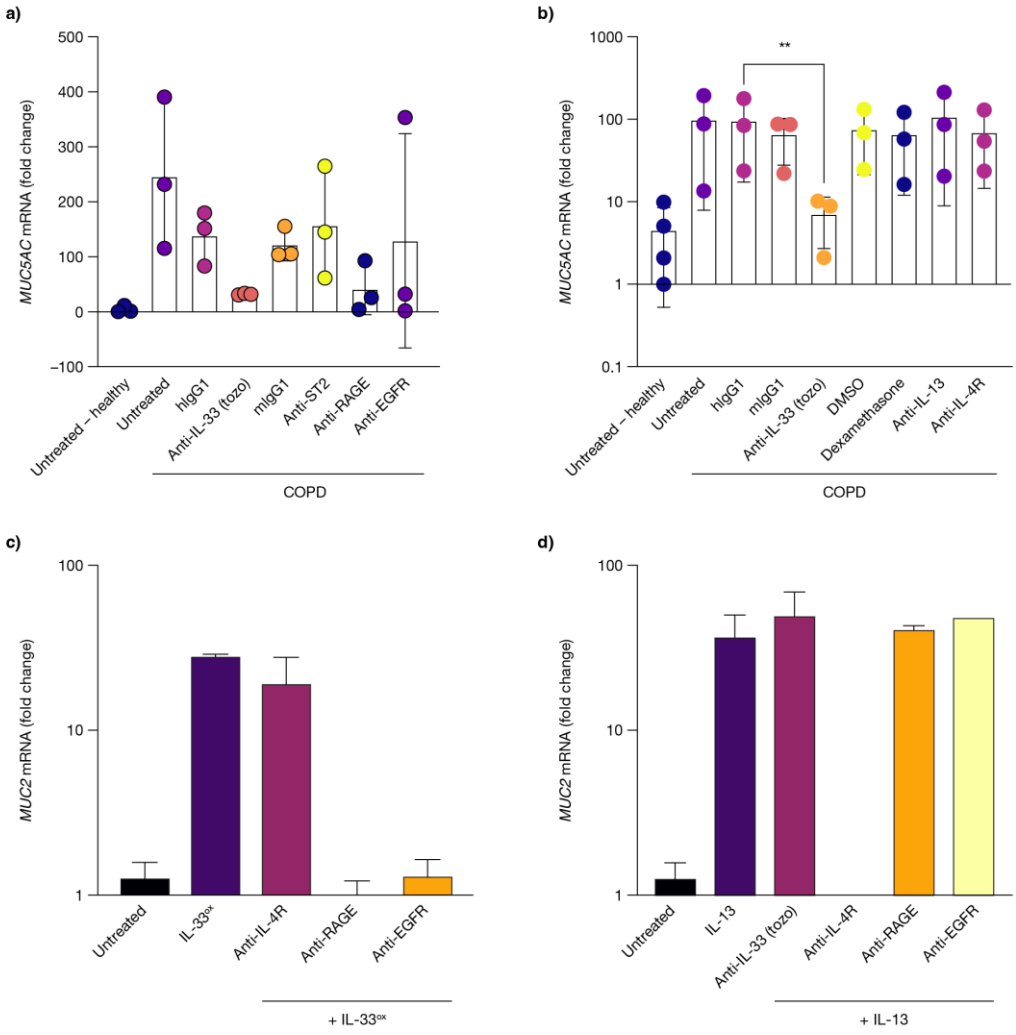
a)
MUC5AC mRNA (fold change)
500
400
300
200
100
0
−100
Untreated – healthy
Untreated
hIgG1
Anti-IL-33 (tozo)
mIgG1
Anti-ST2
Anti-RAGE
Anti-EGFR
COPD
b)
MUC5AC mRNA (fold change)
1000
100
10
1
0.1
**
Untreated – healthy
Untreated
hIgG1
mIgG1
Anti-IL-33 (tozo)
DMSO
Dexamethasone
Anti-IL-13
Anti-IL-4R
COPD
c)
MUC2 mRNA (fold change)
100
10
1
Untreated
IL-33ox
Anti-IL-4R
Anti-RAGE
Anti-EGFR
+ IL-33ox
d)
MUC2 mRNA (fold change)
100
10
1
Untreated
IL-13
Anti-IL-33 (tozo)
Anti-IL-4R
Anti-RAGE
Anti-EGFR
+ IL-13

Supplementary figure S8 IL-33^{ox} induces transcriptional changes that are distinct from those induced by type 2 cytokines

a) *MUC5AC* expression determined by RT-qPCR in healthy or COPD ALI cultures generated from small airway epithelial cells, incubated with IL-33-neutralising (tozorakimab), ST2-neutralising, RAGE-neutralising or EGFR-neutralising antibody or the relevant isotype control antibody, versus untreated control (three individual healthy and three individual COPD donors). b) As in panel a, except that ALI cultures were generated from bronchial epithelial cells, incubated with tozorakimab, DMSO, dexamethasone, anti-IL-13, anti-IL-4R or the relevant isotype control antibody, versus untreated control (four individual healthy and three individual COPD donors). c) *MUC2* expression determined by RT-qPCR in bronchial epithelial ALI cultures following treatment with IL-33^{ox} or IL-33^{ox} + anti-IL-4R, anti-RAGE or anti-EGFR, or untreated control (two individual healthy donors). d) *MUC2* expression determined by RT-qPCR in bronchial epithelial ALI cultures following treatment with IL-13 or IL-13 + tozorakimab, anti-IL-4R, anti-RAGE or anti-EGFR, or untreated control (two individual healthy donors). In panels a–d, error bars show SEM. **p≤0.01. In panels a and b, single data points from individual donors are shown; data are normalised to one healthy donor in the untreated control group.

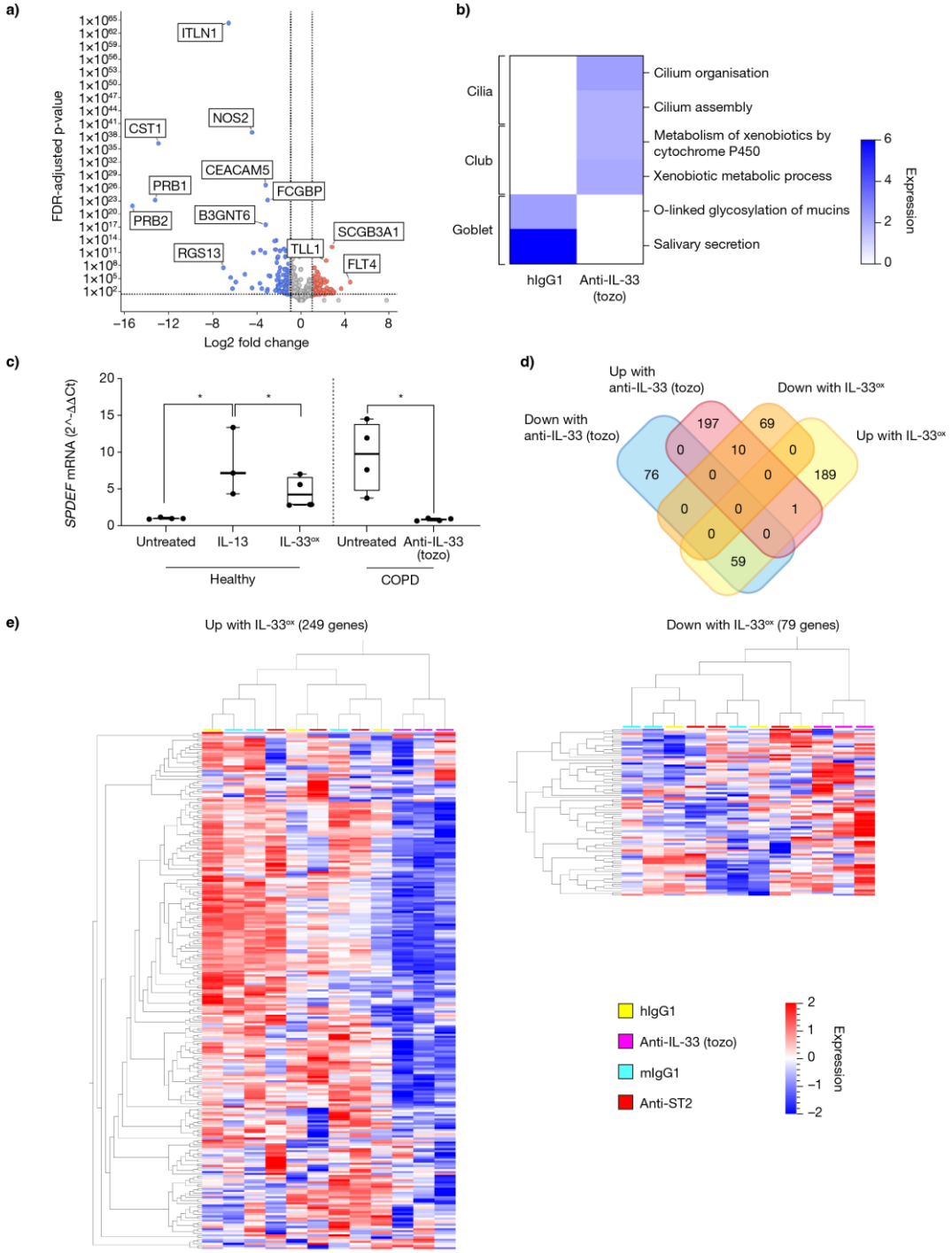
a)
FDR-adjusted p-value
Log2 fold change
ITLN1
NOS2
CST1
CEACAM5
PRB1
FCGBP
PRB2
B3GNT6
SCGB3A1
RGS13
TLL1
FLT4
b)
Cilia
Club
Goblet
Cilium organisation
Cilium assembly
Metabolism of xenobiotics by cytochrome P450
Xenobiotic metabolic process
O-linked glycosylation of mucins
Salivary secretion
hIgG1
Anti-IL-33 (tozo)
Expression
c)
SPDEF mRNA (2^-ΔΔCt)
Untreated
IL-13
IL-33ox
Untreated
Anti-IL-33 (tozo)
Healthy
COPD
d)
Up with anti-IL-33 (tozo)
Down with IL-33ox
Down with anti-IL-33 (tozo)
Up with IL-33ox
197
69
10
76
189
59
e)
Up with IL-33ox (249 genes)
Down with IL-33ox (79 genes)
hIgG1
Anti-IL-33 (tozo)
mIgG1
Anti-ST2
Expression

Supplementary figure S9 Reciprocal gene expression profiles are apparent following anti-IL-33 treatment of COPD ALI cultures and IL-33^{ox} treatment of healthy bronchial epithelial ALI cultures

a) Volcano plot representing differential expression of genes from bulk RNA sequencing in COPD ALI cultures treated with IL-33-neutralising antibody (tozorakimab). b) Heat map showing changes in gene expression levels in COPD ALI cultures following treatment with hIgG1 isotype control antibody or tozorakimab by gene families. c) Expression levels of *SPDEF* in untreated healthy ALI cultures and those treated with IL-13 or IL-33^{ox}, and COPD ALI cultures treated with tozorakimab or isotype control (n=3–4 donors). d) Venn diagram showing overlapping expression profile of genes upregulated with IL-33^{ox} in healthy ALI cultures and genes downregulated with tozorakimab in COPD ALI cultures (greater than twofold change and 0.05 adjusted p-value [Benjamini–Hochberg false discovery rate]). e) Heat maps showing transcriptional changes in COPD ALI cultures after treatment with tozorakimab, ST2-neutralising or the relevant isotype control antibody.

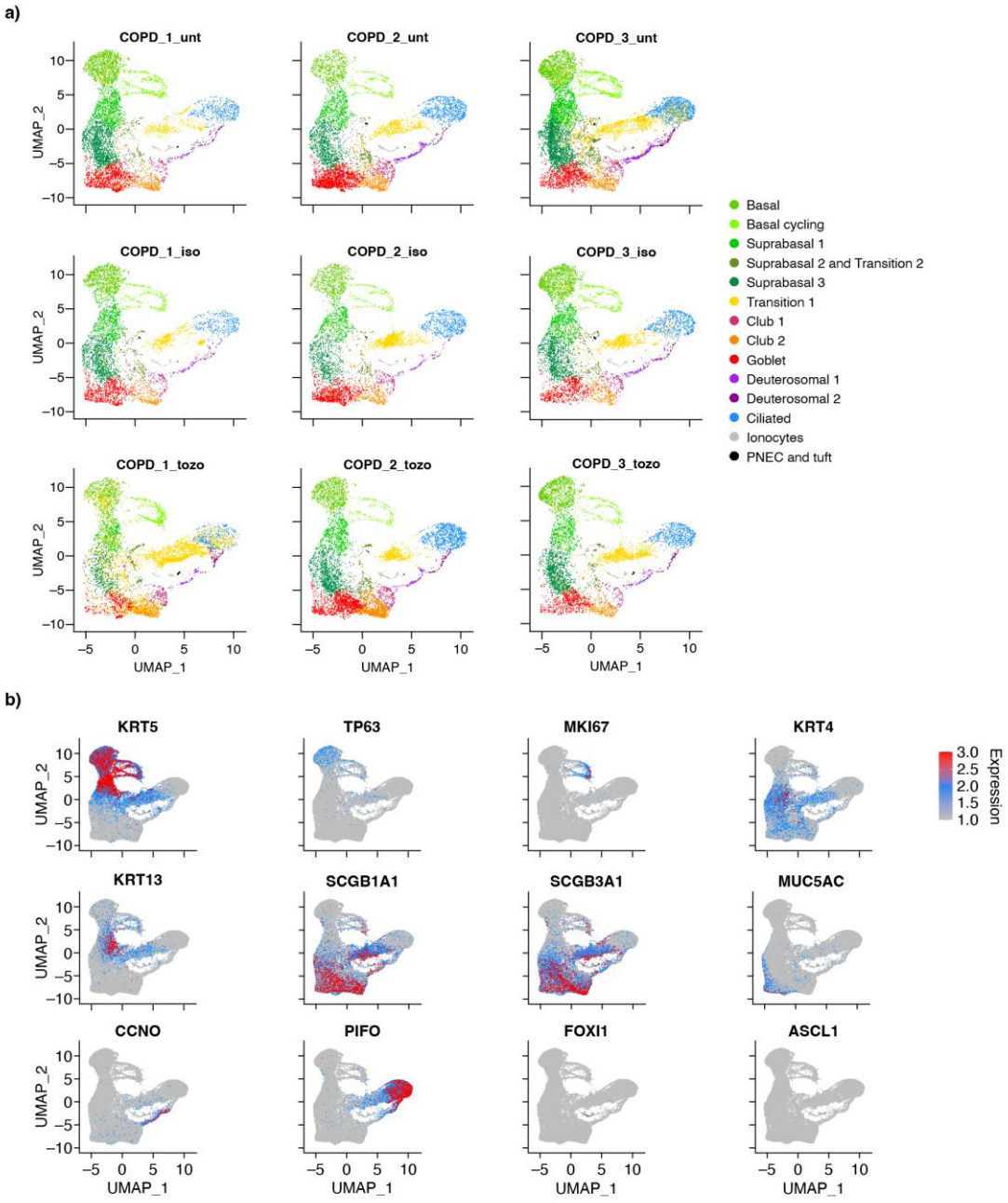
a)
COPD_1_unt
COPD_2_unt
COPD_3_unt
COPD_1_iso
COPD_2_iso
COPD_3_iso
COPD_1_tozo
COPD_2_tozo
COPD_3_tozo
UMAP_1
UMAP_2
Basal
Basal cycling
Suprabasal 1
Suprabasal 2 and Transition 2
Suprabasal 3
Transition 1
Club 1
Club 2
Goblet
Deuterosomal 1
Deuterosomal 2
Ciliated
Ionocytes
PNEC and tuft
b)
KRT5
TP63
MKI67
KRT4
KRT13
SCGB1A1
SCGB3A1
MUC5AC
CCNO
PIFO
FOXI1
ASCL1
Expression

Supplementary figure S10 Single-cell transcriptomic confirmation of airway epithelial cell state in COPD bronchial epithelial ALI cultures

a) Single-cell RNA analysis showing proportions of cell states/types in untreated COPD ALI cultures (n=3; 23 390 cells) or after treatment with IL-33-neutralising antibody (tozorakimab) (n=3; 20 6244 cells) or hIgG1 isotype control antibody (n=3; 16 203 cells). b) UMAP plots of COPD ALI cultures depicting known cell markers for distinguished cell states in the airway epithelium.

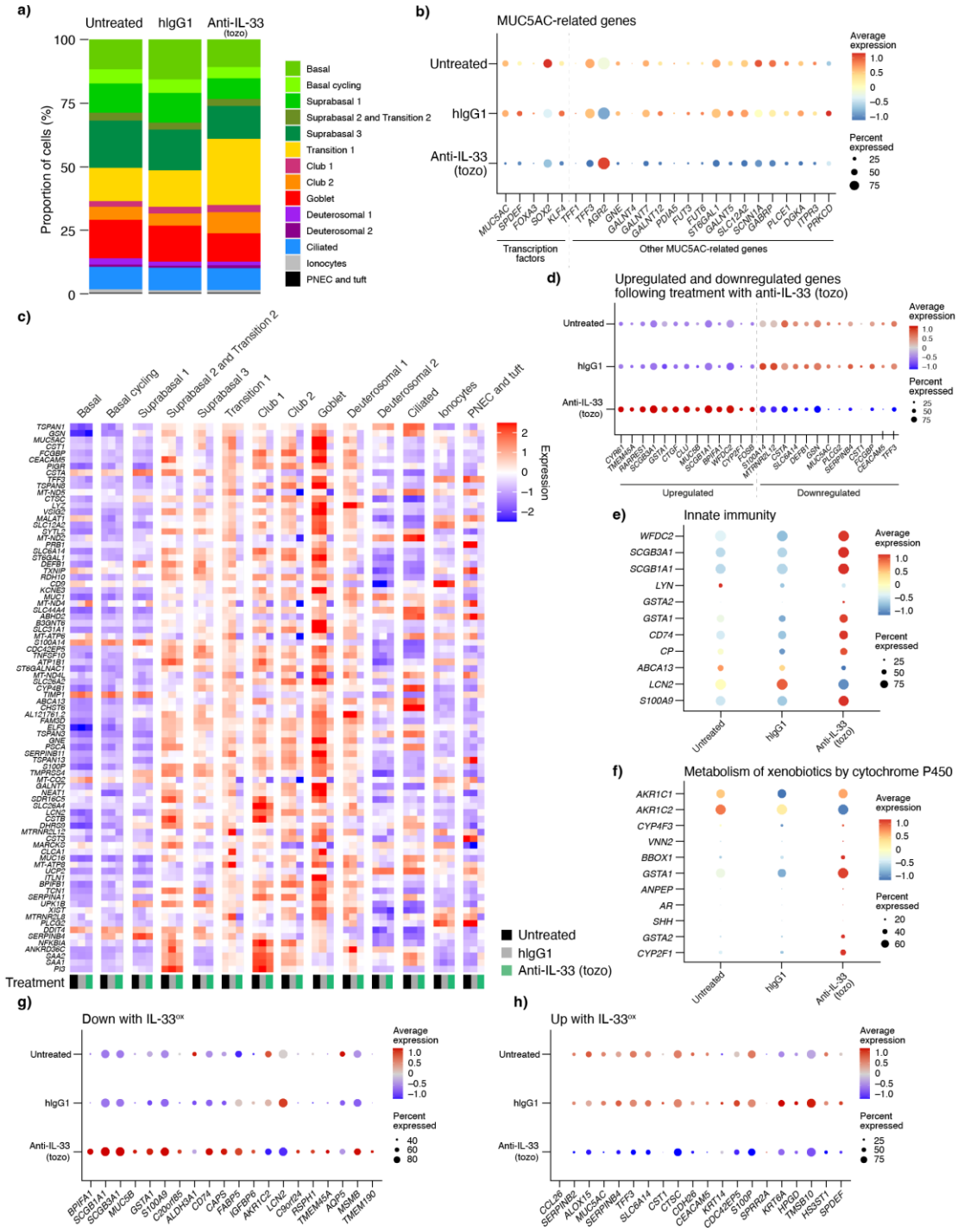
a)
Untreated
hIgG1
Anti-IL-33 (tozo)
Proportion of cells (%)
Basal
Basal cycling
Suprabasal 1
Suprabasal 2 and Transition 2
Suprabasal 3
Transition 1
Club 1
Club 2
Goblet
Deuterosomal 1
Deuterosomal 2
Ciliated
Ionocytes
PNEC and tuft
b)
MUC5AC-related genes
Average expression
Percent expressed
Transcription factors
Other MUC5AC-related genes
c)
Expression
Treatment
Untreated
hIgG1
Anti-IL-33 (tozo)
d)
Upregulated and downregulated genes following treatment with anti-IL-33 (tozo)
Upregulated
Downregulated
e)
Innate immunity
f)
Metabolism of xenobiotics by cytochrome P450
g)
Down with IL-33ox
h)
Up with IL-33ox

Supplementary figure S11 Analysis of inhibition of endogenous IL-33^{ox} in COPD bronchial epithelial ALI cultures using single-cell analysis

a) Stacked bar charts showing changes in cell types identified using single-cell analysis of untreated COPD ALI cultures or after treatment with IL-33-neutralising antibody (tozorakimab) or hIgG1 isotype control antibody. b) Dot plot showing the expression levels of distinct MUC5AC-related genes in COPD ALI cultures treated with tozorakimab or hIgG1 isotype control antibody, or untreated control (n=9; n=3 for each condition). c) Heat map showing changes in gene expression levels measured by single-cell RNA analysis in COPD ALI cultures in the annotated cell states/types following treatment with tozorakimab or hIgG1 isotype control, or untreated control. d) Dot plot showing changes in gene expression identified using single-cell analysis in COPD ALI cultures after treatment with tozorakimab or hIgG1 isotype control antibody, or untreated control. e) Dot plot showing average expressions of genes involved in innate immunity in COPD ALI cultures following treatment with tozorakimab or hIgG1 isotype control, in comparison with untreated controls. f) Dot plot showing average expressions of genes involved in P450 metabolism in COPD ALI cultures following treatment with tozorakimab or hIgG1 isotype control, in comparison with untreated controls. g and h) Dot plots showing scaled expression changes of genes found to be downregulated (g) and upregulated (h) with IL-33^{ox}. In panels b, d, e, f, g and h, the size of the dot represents the percentage of cells expressing the gene.

References

1. Ewels P, Magnusson M, Lundin S, Kaller M. MultiQC: summarize analysis results for multiple tools and samples in a single report. *Bioinformatics* 2016: 32: 3047–3048.

2. Dobin A, Davis CA, Schlesinger F, Drenkow J, Zaleski C, Jha S, Batut P, Chaisson M, Gingeras TR. STAR: ultrafast universal RNA-seq aligner. *Bioinformatics* 2013: 29: 15–21.

3. Gaspar JM. NGmerge: merging paired-end reads via novel empirically-derived models of sequencing errors. *BMC Bioinformatics* 2018: 19: 536.

4. Patro R, Duggal G, Love MI, Irizarry RA, Kingsford C. Salmon provides fast and bias-aware quantification of transcript expression. *Nat Methods* 2017: 14: 417–419.

5. Di Tommaso P, Chatzou M, Floden EW, Barja PP, Palumbo E, Notredame C. Nextflow enables reproducible computational workflows. *Nat Biotechnol* 2017: 35: 316–319.

6. Gruning B, Dale R, Sjodin A, Chapman BA, Rowe J, Tomkins-Tinch CH, Valieris R, Koster J, Bioconda T. Bioconda: sustainable and comprehensive software distribution for the life sciences. *Nat Methods* 2018: 15: 475–476.

7. Love MI, Huber W, Anders S. Moderated estimation of fold change and dispersion for RNA-seq data with DESeq2. *Genome Biol* 2014: 15: 550.

8. Zhu A, Ibrahim JG, Love MI. Heavy-tailed prior distributions for sequence count data: removing the noise and preserving large differences. *Bioinformatics* 2019: 35: 2084–2092.

9. Storey JD, Tibshirani R. Statistical significance for genomewide studies. *Proc Natl Acad Sci USA* 2003: 100: 9440–9445.

10. Hanzelmann S, Castelo R, Guinney J. GSVA: gene set variation analysis for microarray and RNA-seq data. *BMC Bioinformatics* 2013: 14: 7.

11. Steiling K, van den Berge M, Hijazi K, Florido R, Campbell J, Liu G, Xiao J, Zhang X, Duclos G, Drizik E, Si H, Perdomo C, Dumont C, Coxson HO, Alekseyev YO, Sin D, Pare P, Hogg JC, McWilliams A, Hiemstra PS, Sterk PJ, Timens W, Chang JT, Sebastiani P, O'Connor GT, Bild AH, Postma DS, Lam S, Spira A, Lenburg ME. A dynamic bronchial airway gene expression signature of chronic obstructive pulmonary disease and lung function impairment. *Am J Respir Crit Care Med* 2013: 187: 933–942.

12. Tilley AE, O'Connor TP, Hackett NR, Strulovici-Barel Y, Salit J, Amoroso N, Zhou XK, Raman T, Omberg L, Clark A, Mezey J, Crystal RG. Biologic phenotyping of the human small airway epithelial response to cigarette smoking. *PLoS One* 2011: 6: e22798.

13. Tan J, Tedrow JR, Dutta JA, Juan-Guardela B, Nouraie M, Chu Y, Trejo Bittar H, Ramani K, Biswas PS, Veraldi KL, Kaminski N, Zhang Y, Kass DJ. Expression of RXFP1 is decreased in idiopathic pulmonary fibrosis. Implications for relaxin-based therapies. *Am J Respir Crit Care Med* 2016: 194: 1392–1402.

14. Stuart T, Butler A, Hoffman P, Hafemeister C, Papalexi E, Mauck WM, 3rd, Hao Y, Stoeckius M, Smibert P, Satija R. Comprehensive integration of single-cell data. *Cell* 2019: 177: 1888–1902.e1821.

15. Deprez M, Zaragosi L-E, Truchi M, Becavin C, García SR, Arguel M-J, Plaisant M, Magnone V, Lebrigand K, Abelanet S, Brau F, Paquet A, Pe'er D, Marquette C-H, Leroy S, Barbry P. A single-cell atlas of the human healthy airways. *Am J Respir Crit Care Med* 2020: 202: 1636–1645.

16. Jackson ND, Everman JL, Chioccioli M, Feriani L, Goldfarbmuren KC, Sajuthi SP, Rios CL, Powell R, Armstrong M, Gomez J, Michel C, Eng C, Oh SS, Rodriguez-Santana J, Cicuta P, Reisdorph N, Burchard EG, Seibold MA. Single-cell and population transcriptomics reveal pan-epithelial remodeling in type 2-high asthma. *Cell Rep* 2020: 32: 107872.

17. Travaglini KJ, Nabhan AN, Penland L, Sinha R, Gillich A, Sit RV, Chang S, Conley SD, Mori Y, Seita J, Berry GJ, Shrager JB, Metzger RJ, Kuo CS, Neff N, Weissman IL, Quake SR, Krasnow MA. A molecular cell atlas of the human lung from single-cell RNA sequencing. *Nature* 2020: 587: 619–625.

18. Ruiz García S, Deprez M, Lebrigand K, Cavard A, Paquet A, Arguel M-J, Magnone V, Truchi M, Caballero I, Leroy S, Marquette C-H, Marcet B, Barbry P, Zaragosi L-E. Novel dynamics of human mucociliary differentiation revealed by single-cell RNA sequencing of nasal epithelial cultures. *Development* 2019: 146: dev177428.

19. Vieira Braga FA, Kar G, Berg M, Carpaij OA, Polanski K, Simon LM, Brouwer S, Gomes T, Hesse L, Jiang J, Fasouli ES, Efremova M, Vento-Tormo R, Talavera-López C, Jonker MR, Affleck K, Palit S, Strzelecka PM, Firth HV, Mahbubani KT, Cvejic A, Meyer KB, Saeb-Parsy K, Luinge M, Brandsma C-A, Timens W, Angelidis I, Strunz M, Koppelman GH,

van Oosterhout AJ, Schiller HB, Theis FJ, van den Berge M, Nawijn MC, Teichmann SA. A cellular census of human lungs identifies novel cell states in health and in asthma. *Nat Med* 2019: 25: 1153–1163.